# Bone Regeneration by Regulated *In Vivo* Gene Transfer Using Biocompatible Polyplex Nanomicelles

Keiji Itaka[1], Shinsuke Ohba[1], Kanjiro Miyata[2], Hiroshi Kawaguchi[3], Kozo Nakamura[3], Tsuyoshi Takato[3], Ung-Il Chung[1] and Kazunori Kataoka[1,2]

*[1]Division of Clinical Biotechnology, Center for Disease Biology and Integrative Medicine, Graduate School of Medicine, The University of Tokyo, Tokyo, Japan; [2]Department of Materials Science and Engineering, Graduate School of Engineering, The University of Tokyo, Tokyo, Japan; [3]Division of Sensory and Motor System Medicine, Faculty of Medicine, The University of Tokyo, Tokyo, Japan*

Gene therapy is a promising strategy for bone regenerative medicine. Although viral vectors have been intensively studied for delivery of osteogenic factors, the immune response inevitably inhibits bone formation. Thus, safe and efficient non-viral gene delivery systems are in high demand. Toward this end, we developed a polyplex nanomicelle system composed of poly(ethyleneglycol) (PEG)-block-catiomer (PEG-b-P[Asp-(DET)]) and plasmid DNA (pDNA). This system showed little cytotoxicity and excellent transfection efficiency to primary cells. By the transfection of constitutively active form of activin receptor-like kinase 6 (caALK6) and runt-related transcription factor 2 (Runx2), the osteogenic differentiation was induced on mouse calvarial cells to a greater extent than when poly(ethylenimine) (PEI) or FuGENE6 were used; this result was due to low cytotoxicity and a sustained gene expression profile. After incorporation into the calcium phosphate cement scaffold, the polyplex nanomicelles were successfully released from the scaffold and transfected surrounding cells. Finally, this system was applied to *in vivo* gene transfer for a bone defect model in a mouse skull bone. By delivering *caALK6* and *Runx2* genes from nanomicelles incorporated into the scaffold, substantial bone formation covering the entire lower surface of the implant was induced with no sign of inflammation at 4 weeks. These results demonstrate the first success in *in vivo* gene transfer with therapeutic potential using polyplex nanomicelles.

*Received 31 December 2006; accepted 30 April 2007; published online 5 June 2007. doi:10.1038/sj.mt.6300218*

## INTRODUCTION

Despite bone's capacity to heal spontaneously, bone repair is not always satisfactory. Approximately 5–10% of fractures do not heal well, resulting in delayed union or non-union with considerable morbidity.[1] Critical bone defects after severe trauma, tumor resection, or revision of total joint arthroplasty remain challenging problems. Autologous bone graft is considered the gold standard technique; however, it has shortcomings concerning both quantity (availability of material) and quality (donor site troubles, graft rejection, disease transmission).[2,3] These problems have heightened the need for bone regenerative medicine that uses tissue engineering techniques.[4]

A promising strategy is to combine adequate scaffolds and signals. Although some scaffolds are osteoconductive, no scaffolds invented so far are known to be osteoinductive,[5] because current scaffold materials cannot activate the signals necessary for osteogenesis. For this purpose, the potential of growth and transcriptional factors has been widely recognized.[6,7] Substantial progress has been made in the basic understanding of major osteogenic signaling molecules such as bone morphogenetic proteins (BMPs),[8] Hedgehogs,[9] Runx2,[10] Wnts,[11] and insulin-like growth factors.[12] In particular, recombinant human BMP-2 and BMP-7 have already been approved by the U.S. Food and Drug Administration for restricted clinical use. However, in spite of the remarkable findings on animal studies, clinical trials using BMP devices have not obtained comparable outcomes.[13,14] Problems such as protein stability, inadequate release profile (initial burst effect), or the need for accessory factors may have caused these inconsistent results.[6,15]

Gene therapy is a promising approach to overcome these problems. Compared with exogenous proteins, which require purification, the gene can express these bioactive factors in the native form at the regeneration site.[6] The sustained synthesis of proteins from the delivered gene can facilitate synchronization between the kinetics of signaling receptor expression and bioactive factor availability.[16] In addition, the combined use of two or more osteoinductive factors to constitute a better osteogenic signal can be evaluated with a high degree of flexibility.[17] For this purpose, viral vectors including adenovirus and adeno-associated virus vectors have been intensively studied for the delivery of the osteoinductive cytokines.[17–21] However, when these viral vectors are used, there is concern about inducing immune responses.[22] Indeed, Egermann *et al.* reported that, after a local injection of BMP-2 expressing adenoviral vector to a bone defect area in sheep, bone formation was significantly reduced even at the untreated contralateral defect area, indicating that the immune

*The first two authors contributed equally to this work.*

***Correspondence:*** *Kazunori Kataoka, Department of Materials Science and Engineering, Graduate School of Engineering, The University of Tokyo, 7-3-1 Hongo, Bunkyo-ku, Tokyo 113-0033, Japan. E-mail: kataoka@bmw.t.u-tokyo.ac.jp*

response has a systemic inhibitory effect on bone formation after a single injection of adenovirus.[23]

In this context, safe and efficient non-viral gene delivery systems are in high demand. We recently developed a novel polymer-based gene delivery system that showed excellent capacity for *in vitro* transfection.[24] This system is a polyplex nanomicelle composed of poly(ethyleneglycol) (PEG)-block-polycation (PEG-b-P[Asp-(DET)]): PEG-b-polyasparagine carrying the *N*-(2-aminoethyl)aminoethyl group $(CH_2)_2NH(CH_2)_2NH_2$ as the side chain) and plasmid DNA (pDNA). The complexation of block copolymer and pDNA forms a micellar structure, and its characteristics have been found suitable for gene delivery: a diameter of ~100 nm with a PEG palisade enabling complexes to avoid foreign body recognition while providing increased nuclease resistance, increased tolerance under physiologic conditions, and excellent gene expression in a serum-containing medium.[25–27] In addition, the cationic segment of block copolymer was designed to have the buffering capacity of an acidic environment inside the endosomes as effected by the presence of unprotonated amines under neutral pH. By virtue of these features, we effectively transfected genes to culture cells with almost no cytotoxicity.[24]

We undertook the present study to investigate the feasibility of these polyplex nanomicelles for bone regenerative medicine, including the study of: (i) transfection toward various primary cells for the evaluation of efficiency and safety, (ii) induction of osteogenic differentiation by a foreign gene introduction of osteogenic factors, and (iii) *in vivo* gene transfer to a mouse bone defect model to increase the rate of bone regeneration. As will be shown, this system provides sufficient gene expression in a sustained manner both *in vitro* and *in vivo*, and it thus shows a potential therapeutic effect in a bone defect model.

## RESULTS

### *In vitro* transfection to human synovial cells

To evaluate the feasibility of polyplex nanomicelles for clinical gene therapy, *in vitro* transfection was performed toward human synovial cells derived from patients suffering from rheumatoid arthritis. By evaluating luciferase gene expression on day 2 of transfection, the polyplex nanomicelles that were formed at an optimal nitrogen/phosphate ratio showed gene expressions comparable to those of linear poly(ethylenimine) (LPEI),[28] which is well known to have excellent transfection efficiency (**Figure 1a**). At the optimal nitrogen/phosphate = 80, the polyplex nanomicelles were observed to have small absolute zeta potentials of around +10 mV (**Supplementary Figure S1**). The nanomicelles maintained appreciable gene expression even on day 5, whereas the gene expression of LPEI showed a marked decrease during the same time frame. To investigate this difference, the cytotoxicity was evaluated by a quantitative assay. Consistent with the results of gene expression, LPEI exhibited prominent cytotoxicity time-dependently (**Figure 1b**). The microscopic images following green fluorescence protein (GFP) gene transfection by LPEI showed apparent morphologic change as well as reduced numbers of cells, whereas the polyplex nanomicelles maintained almost normal phenotype concurrently with GFP expression even on day 5 (**Supplementary Figure S2**). Thus, the polyplex

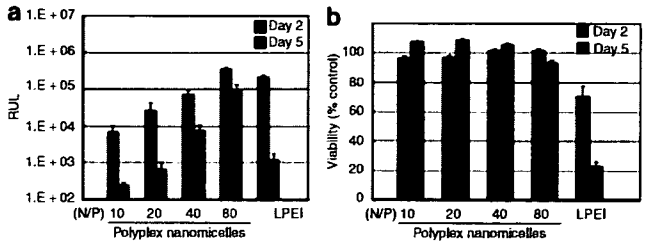


Figure 1 *In vitro* transfection to human synovial cells. (**a**) Luciferase gene expression. *In vitro* transfection of luciferase-expressing plasmid DNA was performed by polyplex nanomicelles formed at various nitrogen/phosphate (N/P) ratios and by poly(ethylenimine) (LPEI). Gene expression was evaluated after 2 and 5 days of transfection. Data are means ± SDs, $n = 4$. (**b**) Cell viability after transfection. After transfection, similar to the case in **a**, cell viability was estimated by an MTT assay. Results were expressed as the relative value (%) of the control cells, which were incubated in parallel without transfection. Data are means ± SDs, $n = 8$. RLU, relative light units.

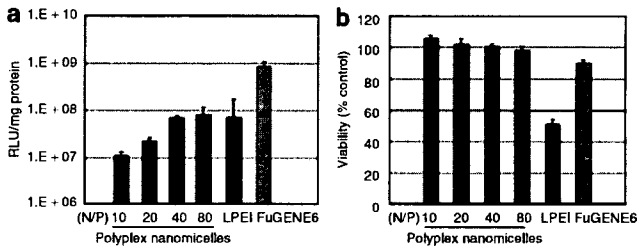


Figure 2 *In vitro* transfection to mouse calvarial cells. (**a**) Luciferase gene expression. *In vitro* transfection of luciferase-expressing plasmid DNA was performed using polyplex nanomicelles, formed at various nitrogen/phosphate (N/P) ratios, as well as poly(ethylenimine) (LPEI) and FuGENE6. Gene expression was evaluated after 2 days of transfection. Data are means ± SDs, $n = 4$. (**b**) Cell viability after transfection. After transfection, similar to the case in **a**, cell viability was estimated by an MTT assay. Results were expressed as relative values (%) of the control cells, which were incubated in parallel without transfection. Data are means ± SDs, $n = 8$. RLU, relative light units.

nanomicelles were revealed to have excellent gene transfection capacity—comparable to that of LPEI—with considerably low cytotoxicity; this suggests a great advantage for *in vivo* application.

### Transfection toward mouse calvarial cells and induction of osteogenic differentiation

In applying polyplex nanomicelles to delivery genes encoding bioactive factors that activate signals necessary for osteogenesis, we evaluated the transfection capacity of foreign genes and the induction of cell differentiation toward mouse calvarial cells derived from neonatal calvariae. The evaluation of luciferase showed that gene expressions comparable to those of LPEI were obtained by polyplex nanomicelles (**Figure 2a**) without showing any cytotoxicity (**Figure 2b**). From a practical standpoint we also evaluated FuGENE6, a commercially available lipid-based transfection reagent with considerably high efficiency and biocompatibility.[29–33] With this reagent, the cells showed luciferase expression that was one order higher than with polyplex nanomicelles or LPEI and with little cytotoxicity (**Figure 2a** and **b**).

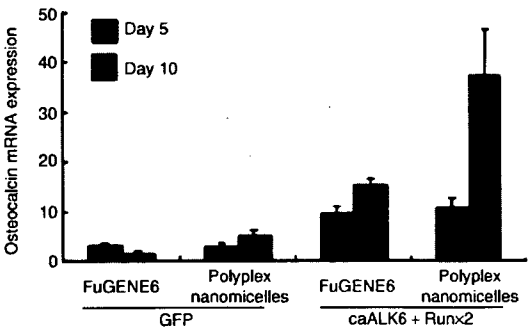


Figure 3 Evaluation of osteocalcin messenger RNA (mRNA) expression by a quantitative polymerase chain reaction (PCR). Osteogenic differentiation was induced on the mouse calvarial cells by transfection of caALK6 and Runx2 expressing plasmid DNAs. As a negative control, a green fluorescence protein (GFP) gene was also used. After 5 and 10 days, the total RNA was collected and the osteocalcin expression was quantified by a quantitative PCR. Data are means ± SDs, $n = 6$. caALK6, constitutively active form of activin receptor-like kinase 6; Runx2, runt-related transcription factor 2.

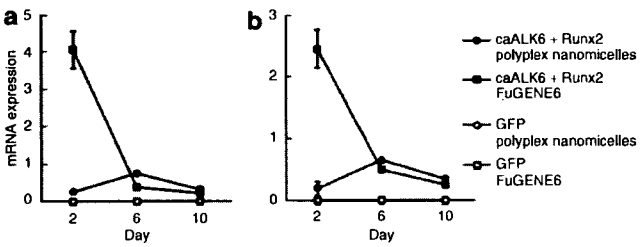


Figure 4 Evaluation of messenger RNA (mRNA) expression of (**a**) constitutively active form of activin receptor-like kinase 6 (caALK6) and (**b**) runt-related transcription factor 2 (Runx2) after transfection by a quantitative polymerase chain reaction. Two, six and ten days after transfection, the mRNA expression of ALK6 and Runx2 was quantified. Data are means ± SDs, $n = 6$. caALK6, constitutively active form of activin receptor-like kinase 6; GFP, green fluorescence protein; Runx2, runt-related transcription factor 2.

Observation of GFP expression revealed that nanomicelles and FuGENE6 achieved similar levels of gene expression without showing any morphologic changes in the cells; this is evident in the phase contrast images (**Supplementary Figure S3**).

We then investigated the osteogenic differentiation after transfection of pDNAs expressing a constitutively active form of activin receptor-like kinase 6 (caALK6) and runt-related transcription factor 2 (Runx2), which have been shown to be a potent combination of genes for bone regeneration.[34] Osteogenic differentiation was evaluated by the expression of osteocalcin messenger RNA (mRNA), an osteoblast-differentiation marker. As shown in **Figure 3**, the time-dependent increase in osteocalcin expression was confirmed after transfection of caALK6 + Runx2 by both polyplex nanomicelles and FuGENE6. Using LPEI, in contrast, osteocalcin expression was at the same level as the control cells transfected with the GFP gene (data not shown). It is interesting that, on day 10, nanomicelles showed a more remarkable increase in osteocalcin expression than did FuGENE6, although both showed comparable gene expression without cytotoxicity by the luciferase and GFP reporter assays (**Figure 2a** and **b** and

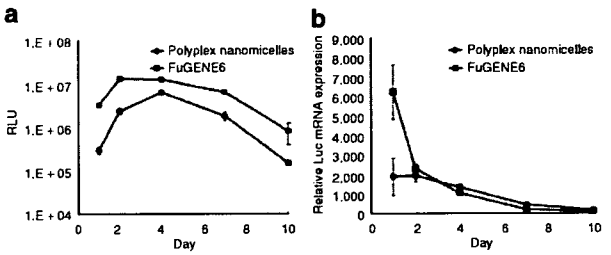


Figure 5 Evaluation of sustained expression of luciferase on mouse calvarial cells. (**a**) Luciferase expression measured by luminescence, which indicated the quantification of protein synthesis. Data are means ± SDs, $n = 12$. (**b**) Estimation of the corresponding messenger RNA (mRNA) expression by a quantitative polymerase chain reaction. For both, the mouse calvarial cells were transfected by luciferase-expressing plasmid DNA and the assays were done on days 1, 2, 4, 7, and 10. Data are means ± SDs, $n = 6$. RLU, relative light units.

**Supplementary Figure S3**). It is reasonable to assume that, with the same transfection procedure as used with the reporter genes, *caALK6* and *Runx2* were also expressed similarly by nanomicelles and FuGENE6. The reasons for this disparity in osteocalcin induction are unclear, but FuGENE6 may cause some appendant effect on cell differentiation that is difficult to detect by a nonspecific viability evaluation such as the MTT assay.[35] Regarding this concern we speculated that, since the difference was visible on day 10, the expression profile of the transfected genes might differ between nanomicelles and FuGENE6, thus affecting the outcome of the induction of cell differentiation.

To investigate this possibility, the time-dependent change of gene expression was quantified. As shown in **Figure 4**, the mRNA expressions of caALK6 and Runx2 showed similar profiles, where FuGENE6 initially induced expressions of ALK6 and Runx2 that were one order higher than nanomicelles, although the expressions sharply decreased with time. In contrast, the nanomicelles showed rather consistent gene expressions. For a detailed investigation, the luciferase gene was used and the protein systhesis and its mRNA expression were simultaneously quantified by a luminescence measurement and a quantitative polymerase chain reaction (PCR), respectively. As shown in **Figure 5**, FuGENE6 initially showed light emission (indicating the amount of synthesized protein) that was one order higher than did the nanomicelles. The highest expression was obtained on day 2. The initial mRNA expression was always high, but a rapid decrease was observed after day 2. In contrast, the polyplex nanomicelles showed fairly consistent gene expression profiles, giving the highest luciferase expression on day 4 and with sustained mRNA expression thereafter. Because cell differentiation would require some processes in signaling pathways inside the cells, it follows that such a continuous manner of gene expression by polyplex nanomicelles might contribute to the efficient induction of differentiation. Hence, the nanomicelle profile is a promising feature for *in vivo* bone regeneration.

### *In vitro* transfection from gene-containing scaffolds

The *in vivo* gene transfer to a bone regeneration site should require the retention and gradual release of gene carriers. One promising approach is to incorporate the carriers into implantable scaffolds.

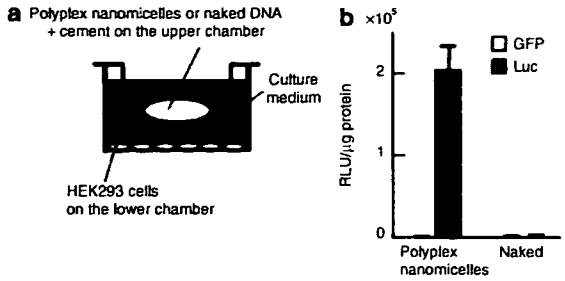


Figure 6 *In vitro* transfection by polyplex nanomicelles incorporated into calcium phosphate cement scaffold. (**a**) Schematic illustration of the *in vitro* transfection from the gene-containing scaffolds. The scaffold containing polyplex nanomicelles of PEG-b-P[Asp-(DET)] and plasmid DNA (pDNA) expressing luciferase gene or naked pDNA was plated onto the upper chamber of cell culture insert, and the HEK293 cells were plated onto the lower chamber. (**b**) Luciferase expression in HEK293 cells. After 5 days of transfection, luciferase expression was measured. The green fluorescence protein (GFP) gene was used as a negative control. Data are means ± SDs, $n = 3$. DET, diethylenetriamine; PEG, poly(ethyleneglycol); RLU, relative light units.

This form of gene delivery is called the gene-activated matrix, through which Bonadio *et al.* pioneered the incorporation of non-viral vectors in collagen scaffolds to stimulate bone formation in a rat defect model.[36] In this study, the polyplex nanomicelles were incorporated into a calcium phosphate cement scaffold by mixing. This process is highly biocompatible, bioactive (especially in bone tissue), moldable, and injectable.

In order to investigate whether or not the polyplex nanomicelles containing luciferase-expressing pDNA were delivered from the calcium phosphate cement scaffold, the scaffold was put into the culture medium of HEK293 cells for 5 days. The cement and the cells were physically separated by a filter to avoid direct contact between the cement and the cells, which could hinder the distinction between the release and the direct delivery of polyplex nanomicelles from the scaffold (**Figure 6**). As shown in **Figure 6b**, the cells cultured with the scaffold containing the polyplex nanomicelles exhibited apparent luciferase expression, whereas the cells cultured with the scaffold containing naked pDNA did not. Thus, the polyplex nanomicelles incorporated into the calcium phosphate cement scaffold successfully introduced the contained genes into the surrounding cells.

Next, to investigate how long the transfection by polyplex nanomicelles incorporated into the scaffold would last, the scaffold was placed on the culture dish and then mouse calvarial cells were plated on top of it and cultured for an extended period. Monitoring of luminescence using the IVIS Imaging System (Xenogen, Alameda, CA) revealed that the gene expression of mouse calvarial cells by the scaffold containing polyplex nanomicelles with luciferase-expressing pDNA increased, peaking near days 10 and 18, and then gradually declined to the background level approaching day 25 (**Supplementary Figure S4a**). Quantitative visualization of luminescence using this imaging system revealed that cells on top of the scaffold and in its close proximity were first transfected at days 2 and 10; subsequently, cells at some distance were transfected until day 25 (**Supplementary Figure S4b**). Thus, the polyplex nanomicelles incorporated into the scaffold delivered genes in a sustained manner.

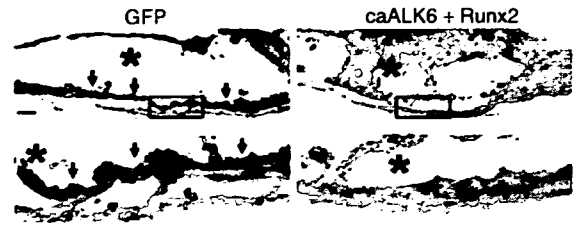


Figure 7 *In vivo* gene transfer by polyplex nanomicelles. Immunohistochemistry for green fluorescence protein (GFP) of calvarias implanted with the scaffold containing polyplex nanomicelles of PEG-b-P[Asp-(DET)] and plasmid DNA expressing GFP or caALK6 + Runx2 at 4 weeks after implantation. GFP protein was stained brown (arrows). The lower panel of each group shows a magnified view of the boxed area in the upper panel. Asterisks denote the remnants of calcium phosphate pastes. Scale bar: 200 μm. caALK6, constitutively active form of activin receptor-like kinase 6; DET, diethylenetriamine; PEG, poly(ethyleneglycol); Runx2, runt-related transcription factor 2.

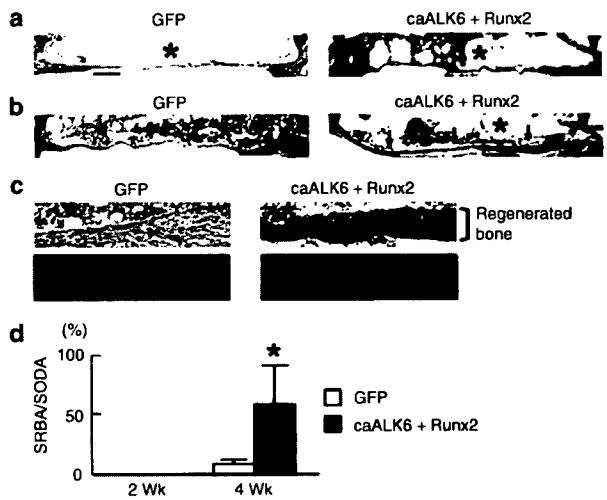


Figure 8 Bone regeneration by polyplex nanomicelles. (**a**, **b**) Histologic analyses of calvarias. The scaffold containing polyplex nanomicelles of PEG-b-P[Asp-(DET)] and plasmid DNA expressing green fluorescence protein (GFP) or caALK6 + Runx2 was implanted on the bone defect area on the mouse skull bone. At (**a**) 2 weeks and (**b**) 4 weeks after implantation, histologic and immunohistologic analyses were performed. Sections were stained with hematoxylin and eosin (H&E). Arrowheads denote defect edges; arrows, regenerated bones; asterisks, the remnants of calcium phosphate cement. Scale bar: 500 μm. (**c**) Magnified views of boxed areas in **b**. H&E (bright field views) and immunohistochemstry for type-I collagen (dark field views) were performed on serial sections. Green fluorescence indicates expression of type-I collagen. Asterisks, the remnants of calcium phosphate cement. (**d**) Quantification of bone regeneration. The ratio of the summation of the regenerated bone area to that of the original defect area (SRBA/SODA) in designated sections was histologically measured by NIH Image software. Data are means ± SD of five mice per group. $^*P < 0.01$ versus GFP at 4 weeks after implantation. caALK6, constitutively active form of activin receptor-like kinase 6; DET, diethylenetriamine; PEG, poly(ethyleneglycol); Runx2, runt-related transcription factor 2.

## *In vivo* gene delivery to the bone defect area on the mouse calvarial bone

The data so far have shown that a localized and sustained system to deliver polyplex nanomicelles was successfully developed *in vitro* using the calcium phosphate cement scaffold. To

investigate whether or not this system is effective for *in vivo* gene delivery, the scaffold was molded to the fitting shape and implanted in mouse calvarial bone defects. After implantation of the scaffold containing polyplex nanomicelles with GFP pDNA, successfully transfected recipient cells were observed across a few layers from the implant surface by immunohistochemical analyses (**Figure 7**). The intensity of the staining was strongest in cells immediately adjacent to the scaffold, gradually declining with distance.

To investigate the therapeutic potential of this system, polyplex nanomicelles containing pDNAs expressing a caALK6 and Runx2, by which the osteogenic differentiation was induced on the calvarial cells *in vitro* (**Figure 3**), were incorporated into the calcium phosphate cement scaffold and implanted in the same model. At 2 weeks after implantation, no bone formation occurred in either the control group transfected with the GFP-expressing pDNA or the treatment group transfected with caALK6 + Runx2 expressing pDNA (**Figure 8a**). At 4 weeks after implantation, however, substantial bone formation covering the entire lower surface of the implant was induced only in the treatment group (**Figure 8b**), as confirmed by the quantitative analysis of the regenerated bone area (**Figure 8d**). The regenerated bone tissues exhibited a lamellar structure containing osteocyte-like cells and strongly expressed the type-I collagen protein (**Figure 8c**). On the other hand, the incorporation of neither the LPEI nor the FuGENE6 complex into the calcium phosphate cement scaffold generated any apparent bone formation at 4 weeks (data not shown). It should be noted that no sign of inflammation was observed in any group (**Figure 8a–c**). The results so far indicate that the polyplex nanomicelles incorporated into the calcium phosphate cement scaffold transfected the foreign genes to the cells in the vicinity of the scaffold, leading to a considerable increase in the rate of bone formation via the induction of osteogenic differentiation.

## DISCUSSION

Many clinical fields demand useful non-viral gene delivery systems that satisfy high standards of both efficacy of gene introduction and low toxicity.[37] Bone tissue engineering would be a promising field; however, only a few trials have been reported so far. Bright *et al.* used a naked pDNA expressing OP-1 (BMP-7) gene, which was incorporated into a collagen scaffold, for a rat model of lumbar interbody arthrodesis.[38] Although bone formation was stimulated after 4 weeks, it was not as extensive as that observed after the injection of recombinant human OP-1 protein, in spite of considerably high dose of pDNA (250 μg/rat). Huang *et al.* combined poly(lactic-co-glycolic acid) scaffolds with 200 μg of condensed pDNA encoding BMP4 using branched PEI and implanted the scaffolds into rat cranial defects.[39] They successfully induced bone regeneration at the defect edges; however, osteoid and mineralized tissue was significantly increased after 15 weeks of implantation. The disparity between our results and theirs presumably resulted from the difference in the osteogenic signals. However, some toxic effects of PEI should also be taken into consideration: PEI was reported to be an apoptotic agent,[40] and indeed in our results it showed appreciable cytotoxicity (**Figures 1b and 2b**) and an inability to induce differentiation. Directly comparing the capacity of their versus our method was not possible because Huang *et al.* did not provide data on the actual transfection efficiency; however, some negative effects of PEI on the cells in the vicinity of the scaffold may have caused the delayed induction of bone regeneration.

The considerably low dose of pDNA (1.3 μg/mouse) is also characteristic in our system. In previous studies of *in vivo* bone formation by non-viral gene delivery systems, a larger amount of pDNA (100 μg to 1 mg) was used.[38,39,41] We assume that this may be attributed to the capacity of polyplex nanomicelles to stably retain pDNA even in the scaffolds. Moreover, using the combination of osteogenic genes *caALK6* and *Runx2* contributed to the efficient osteoconductivity of our system. The cooperative action of this combination occurred through protein stabilization of core binding factor beta (Cbfb) and through induction of Runx2–Cbfb complex formation and its DNA binding, leading to the efficient induction of osteogenic differentiation.[34]

FuGENE6 has often been reported to have excellent transfection efficiency *in vitro*, including the induction of cell differentiation.[29–33] Indeed, in our results shown in **Figure 3**, comparable induction of osteocalcin expression was observed by both FuGENE6 and polyplex nanomicelles on day 5. It is interesting to note that, although the gene expressions evaluated by luciferase were consistently higher in FuGENE6 until day 10 (**Figure 5**), the osteocalcin induction was more remarkable in the nanomicelles on day 10 (**Figure 3**). The marked difference in gene expression profiles between nanomicelles and FuGENE6—especially when evaluated by mRNA expression—might influence the outcome of cell differentiation, which requires complex intracellular processes over an extended period. It is also possible that some toxicologic effects of the reagents might influence the cell reactivity, since many lipid-based transfection reagents were reported to induce changes in the expression of endogenous genes.[42] The study of toxicologic or pharmacologic effects of bioactive materials that might alter responses to delivered drugs or genes is now attracting attention as polymer (material) genomics.[43] From this standpoint, we have started comprehensive analyses of cell bioactivities after various transfection procedures, including the study of endogenous gene expression profiles using complementary DNA arrays. These results will be reported elsewhere in the near future.

The polyplex nanomicelles composed of PEG-b-P[Asp-(DET)] block copolymer and pDNA have demonstrated promising features for bone-regenerative gene therapy. The characteristics are summarized as: (i) good transfection efficiency with minimal cytotoxicity; (ii) sustained gene expression profile, which may be beneficial to cell differentiation; and (iii) excellent *in vivo* availability. Worth noting is that the enhancement of bone regeneration in this study was achieved without cell transplantation. Although the use of cell sources such as stem cells has been widely investigated, there remain many concerns for clinical application, such as the difficulty of finding an ideal cell source that meets both quality and quantity demands while also satisfying the concerns of medical costs and health risks.[44,45] Thus, it is desirable that cell transplantation be supplemented or replaced by innovations in other components of tissue engineering, signals, and scaffolds.

In conclusion, we developed a new gene delivery system applicable to bone regenerative medicine. This polyplex nanomicelle showed high biocompatibility as well as a capacity for regulated gene transfer, inducing a remarkable increase in the bone regeneration rate in a bone defect model. This system holds much promise for constructing a practical gene-activated matrix for tissue engineering. Moreover, this technology will help realize therapeutic applications of gene therapy requiring safe and regulated gene expressions.

## MATERIALS AND METHODS

***Materials.*** pDNAs encoding luciferase (pGL3-control, 5,256 bp) (Promega, Madison, WI) and GFP (pEGFP-C1, 4,700 bp) (Clontech, Palo Alto, CA) were amplified in competent DH5α *Escherichia coli* and purified using EndoFree Plasmid Maxi or Mega Kits (Qiagen, Hilden, Germany). pCMV5 pDNA expressing hemagglutinin-tagged mouse caALK6 and pcDEF3 pDNA expressing Flag-tagged mouse Runx2 were generous gifts from M. Krüppel (Mt. Sinai Hospital, Toronto, Canada) and K. Miyazono (University of Tokyo, Tokyo, Japan), respectively. The DNA concentration was determined by reading the absorbance at 260 nm. Commercially available transfection reagents, linear polyethylenimine (Exgen 500, $M_w$ of LPEI = 22 kd) and FuGENE6 were purchased from MBI Fermentas (Burlington, Canada) and Roche (Basel, Switzerland), respectively. Dulbecco's modified Eagle's medium and fetal bovine serum were purchased from Sigma-Aldrich (St. Louis, MO).

***Synthesis and characterization of PEG-b-P[Asp-(DET)] block copolymer.*** The PEG-b-P[Asp-(DET)] block copolymer was synthesized as previously reported.[24] Briefly, PEG-poly(β-benzyl-L-aspartate) (PEG-PBLA) diblock copolymer was synthesized by the ring-opening polymerization of β-benzyl-L-aspartate *N*-carboxy-anhydride from the terminal primary amino group of α-methoxy-ω-amino PEG ($M_w$: 12,000; Nippon Oil and Fats, Tokyo, Japan). The copolymer thus prepared was confirmed to be unimodal with a narrow molecular weight distribution ($M_w/M_n$: 1.23) by gel-permeation chromatography, and the number of repeating units of BLA was calculated to be 68 by $^1$H-NMR (data not shown). The N-terminal amino group of PEG-PBLA was then acetylated using acetic anhydride in dichloromethane solution to obtain PEG-PBLA-Ac. The obtained polymer was dissolved in distilled *N,N*-dimethylformamide (Wako Pure Chemical Industries, Osaka, Japan) and reacted with diethylenetriamine (DET) (Tokyo Kasei Kogyo, Tokyo, Japan) for 24 hours at 40 °C under a dry argon atmosphere to undergo aminolysis of the benzyl side chain. After 24 hours, the solution was slowly dropped into 10% acetic acid solution and dialyzed (Spectra/por Membrane, molecular weight cut-off = 3,500, Rancho Dominquez, CA) against 0.01 N HCl and subsequently against distilled water. The final solution was lyophilized to obtain PEG-b-P[Asp-(DET)] as the hydrochloride salt form. $^1$H-NMR confirmed the complete substitution of benzyl ester of the polymer with DET through the aminolysis reaction as well as the chemical structure of the obtained PEG-b-P[Asp-(DET)] block copolymer.

***Preparation of pDNA carriers.*** The PEG-b-P[Asp-(DET)] block copolymer and pDNA were separately dissolved in 10 mmol/l Tris–HCl buffer (pH 7.4). Both solutions were mixed at various nitrogen/phosphate (= (total amines in cationic segment)/(DNA phosphates)) and left overnight. The pDNA complexes with LPEI and FuGENE6 were prepared by mixing the pDNA solution and the reagents following the protocols provided by the manufacturers.

**In vitro *transfection.*** HEK293 cells were obtained from the Riken Cell Bank (Tsukuba, Japan). Mouse calvarial cells were isolated from calvariae of neonatal littermates. The experimental procedures were in accordance with the guidelines of the Animal Committee of the University of Tokyo. Calvariae were digested for 10 minutes at 37 °C in an enzyme solution containing 0.1% collagenase and 0.2% dispase for five cycles. Cells isolated by the final four digestions were combined as an osteoblast population and cultured in Dulbecco's modified Eagle's medium containing 10% fetal bovine serum. Human synovial cells from rheumatoid arthritis patients were kindly provided by Dr. S. Tanaka (University of Tokyo).[46] Written informed consent for subsequent experiments was obtained from each patient.

For luciferase transfection assays, the cells were inoculated at a density of $2 \times 10^4$ cells/well in a 24-multiwell plate and cultured for 24 hours. After the culture medium was replaced with fresh medium containing 10% fetal bovine serum, pDNA carrier solution (33.3 μg/ml, 22.5 ml) was applied to each well. After several days of incubation, the cells were lysed and the luciferase gene expression was measured using a Luciferase Assay System (Promega, Madison, WI) and a Lumat LB9507 luminometer (Berthold, Bad Wildbad, Germany). The expression was normalized to protein concentrations of cell lysates. For the evaluation of sustained luciferase expression (**Figure 4**), the cells were seeded onto a 96-multiwell plate ($6 \times 10^3$ cells/well). After incubation for 24 hours, 6 μl of each pDNA carrier solution was added, followed by further incubation for up to day 10. The luminescence was measured by a GloMax 96 Microplate Luminometer (Promega, Madison, WI). For the GFP transfection assay, both the phase contrast and the fluorescence images were obtained by an Axiovert 100 M microscope (Carl Zeiss, Oberkochen, Germany).

For the cytotoxicity assay, a 96-multiwell plate was used. After transfection as described above, the cells were incubated for 2 or 5 days and their viability was evaluated by an MTT assay (Cell Counting Kit-8, Dojindo, Kumamoto, Japan). Each well was measured by reading the absorbance at 450 nm according to the protocol provided by the manufacturer. The results were expressed as the relative value (%) of the control cells, which were incubated in parallel without transfection.

***Evaluation of mRNA expression.*** After transfection to mouse calvarial cells, the total RNA was collected using the RNeasy Mini Preparation Kit (Qiagen, Hilden, Germany) according to the manufacturer's protocol. Gene expression was analyzed by quantitative PCR. Using the Quantitect SYBR Green PCR Kit (Qiagen, Hilden, Germany), 20 ng of total RNA was analyzed in a final volume of 20 μl according to the manufacturer's protocol. Reverse transcription was performed for 30 minutes at 50 °C followed by PCR: 40 thermal cycles of 15 seconds at 94 °C, 30 seconds at 55 °C, and 30 seconds at 72 °C using an ABI Prism 7500 Sequence Detector (Applied Biosystems, Foster City, CA). Each mRNA expression was normalized to levels of mouse β-actin mRNA, also determined by quantitative reverse transcription-PCR, from the same total RNA samples. The following primers were used: osteocalcin, forward primer (AAGCAGGAGGGC AATAAGGT) and reverse primer (TTTGTAGGCGGTCTTCAAGC); mouse ALK6, forward primer (CACCAAGAAGGAGGATGGAG) and reverse primer (CTAGACATCCAGAGGTGACAACAG); mouse Runx2, forward primer (CCCAGCCACCTTTACCTACA) and reverse primer (TATGGAGTGCTGCTGGTCTG); luciferase, forward primer (TTGA CCGCCTGAAGTCTCTGA) and reverse primer (ACACCTGCGTCGA AGATGTTG); mouse β-actin, forward primer (AGATGTGGATCAG CAAGCAG) and reverse primer (GCGCAAGTTAGGTTTTGTCA). As for luciferase, the gene expression presented as the light units was also evaluated in parallel.

**In vitro *transfection from gene-containing scaffolds.*** To prepare the scaffolds containing gene carriers, the PEG-P[Asp-(DET)]/pDNA micelles were mixed with calcium phosphate paste (BIOPEX-R; Mitsubishi Pharma, Osaka, Japan). According to the manufacturer's information, the powder consists of particles (2–5 mm in diameter) of α-tricalcium phosphate (75% wt), tetracalcium phosphate monoxide (18% wt), dicalcium phosphate dibasic (5% wt), and hydroxyapatite (2% wt); the aqueous solution contains sodium chondroitin sulfate (5.4%) and sodium succinate

(13%). For solidification, 1.0 g of the powder was manually mixed (at low shear rates) with 233 µl of the solution containing pDNAs. After solidification, the cement containing 1.3 µg of pDNA was placed onto the upper chamber of a BD Falcon Cell Culture Insert for 12-well plates (1.0 µm pore size, Becton Dickinson, Franklin Lakes, NJ), and HEK293 cells were plated onto the lower chamber. Five days later, luciferase assay was performed as described. The level of luciferase expression was normalized to the protein concentrations of cell lysates.

***In vivo gene delivery for the bone defect area on the mouse skull bone.*** In this study, the 4 mm defects in diameter were chosen as the mouse bone defect model.[47,48] We have observed that the mouse calvarial defects (4 mm in diameter) could not be covered spontaneously with regenerated bone within 8 weeks after operation, although significant bone formation was observed at the defect edge (data not shown). Thus, the bone regeneration was evaluated within or at 4 weeks after gene delivery.

For the generation of bone defects, mice were anesthetized with ketamine/xylazine (80 mg/kg and 5 mg/kg) solution through intraperitoneal injection, and a linear incision was made along the sagittal suture from the frontal bone to the center of the occipital bone. A round craniotomy defect (4 mm in diameter) was manually created on both parietal bones with a sterile disposable trephine (Kai Industries, Gifu, Japan).[47] Calcium phosphate paste was used to fill in the defects, and then the incisions were sutured. The mice were killed at 2, 4, or 8 weeks after the operation for radiologic, histologic, or immunohistologic analyses, respectively. Animal experiments were performed according to the protocol approved by the Animal Care and Use Committee of the University of Tokyo.

***Assessment of bone regeneration.*** After the mice were asphyxiated with carbon dioxide, the calvarias were removed. Tissue preparation, hematoxylin and eosin staining, and immunohistologic analysis using a rabbit polyclonal antibody against GFP (Molecular Probes, Eugene, OR) or a rabbit polyclonal antibody against type-I collagen (LSL, Tokyo, Japan) were performed as described.[49] To evaluate the extent of bone regeneration, serial coronal sections of the implantation site were performed at 0.5, 1, 1.5, 2, 2.5, 3, and 3.5 mm from the rostral end and then stained with hematoxylin and eosin. For each section, the original defect area and the regenerated bone area were measured by NIH Image software. The ratio of the summation of the regenerated bone area to that of the original defect area (SRBA/SODA) was calculated and used as the index of bone regeneration.

## ACKNOWLEDGMENTS

We thank Michael Klüppel (Mount Sinai Hospital) and Kohei Miyazono (University of Tokyo) for pDNAs expressing caALK6 and Runx2, respectively. We also appreciate Sakae Tanaka (University of Tokyo) for providing human synovial cells. This work was supported by Grants-in-Aid for Scientific Research from the Japanese Ministry of Education, Culture, Sports, Science and Technology (#15390452 and #17390530), Health Science Research Grants from the Japanese Ministry of Health, Labor and Welfare (#H16-regenerative medicine-008), and the Core Research Program for Evolutional Science and Technology (CREST) from the Japan Science and Technology Corporation (JST).

## SUPPLEMENTARY MATERIAL

**Figure S1.** Zeta-potential of polyplex nanomicelles and pDNA complexes with P[Asp-(DET)], the cationic segment of the block copolymer used in this study.
**Figure S2.** GFP gene expression in human synovial cells.
**Figure S3.** GFP gene expression in mouse calvarial cells.
**Figure S4.** *In vitro* transfection by polyplex nanomicelles incorporated into calcium phosphate cement scaffold.

## REFERENCES

1. Bucholz, RW, Heckman, JD (2006). *Rockwood and Green's Fractures in Adults*. Lippincott Williams & Wilkins: Philadelphia, PA. 587pp.
2. Banwart, JC, Asher, MA and Hassanein, RS (1995). Iliac crest bone graft harvest donor site morbidity. A statistical evaluation. *Spine* **20**: 1055–1060.
3. Arrington, ED, Smith, WJ, Chambers, HG, Bucknell, AL and Davino, NA (1996). Complications of iliac crest bone graft harvesting. *Clin Orthop Relat Res* **329**: 300–309.
4. Langer, R and Vacanti, JP (1993). Tissue engineering. *Science* **260**: 920–926.
5. Bruder, SP and Caplan, AI (2000). *Principles of Tissue Engineering*. Academic Press: San Diego, CA. 683pp.
6. Winn, SR, Hu, Y, Sfeir, C and Hollinger, JO (2000). Gene therapy approaches for modulating bone regeneration. *Adv Drug Deliv Rev* **42**: 121–138.
7. Baltzer, AW and Lieberman, JR (2004). Regional gene therapy to enhance bone repair. *Gene Ther* **11**: 344–350.
8. Katagiri, T and Takahashi, N (2002). Regulatory mechanisms of osteoblast and osteoclast differentiation. *Oral Dis* **8**: 147–159.
9. Long, F, Chung, UI, Ohba, S, McMahon, J, Kronenberg, HM and McMahon, AP (2004). Ihh signaling is directly required for the osteoblast lineage in the endochondral skeleton. *Development* **131**: 1309–1318.
10. Komori, T (2003). Requisite roles of Runx2 and Cbfb in skeletal development. *J Bone Miner Metab* **21**: 193–197.
11. Patel, MS and Karsenty, G (2002). Regulation of bone formation and vision by LRP5. *N Engl J Med* **346**: 1572–1574.
12. Ogata, N, Chikazu, D, Kubota, N, Terauchi, Y, Tobe, K, Azuma, Y *et al.* (2000). Insulin receptor substrate-1 in osteoblast is indispensable for maintaining bone turnover. *J Clin Invest* **105**: 935–943.
13. Govender, S, Csimma, C, Genant, HK, Valentin-Opran, A, Amit, Y, Arbel, R *et al.* (2002). Recombinant human bone morphogenetic protein-2 for treatment of open tibial fractures: a prospective, controlled, randomized study of four hundred and fifty patients. *J Bone Joint Surg Am* **84-A**: 2123–2134.
14. Valentin-Opran, A, Wozney, J, Csimma, C, Lilly, L and Riedel, GE (2002). Clinical evaluation of recombinant human bone morphogenetic protein-2. *Clin Orthop Relat Res* **395**: 110–120.
15. Gerstenfeld, LC, Cullinane, DM, Barnes, GL, Graves, DT and Einhorn, TA (2003). Fracture healing as a post-natal developmental process: molecular, spatial, and temporal aspects of its regulation. *J Cell Biochem* **88**: 873–884.
16. Howell, TH, Fiorellini, J, Jones, A, Alder, M, Nummikoski, P, Lazaro, M *et al.* (1997). A feasibility study evaluating rhBMP-2/absorbable collagen sponge device for local alveolar ridge preservation or augmentation. *Int J Periodontics Restorative Dent* **17**: 124–139.
17. Zhao, M, Zhao, Z, Koh, JT, Jin, T and Franceschi, RT (2005). Combinatorial gene therapy for bone regeneration: cooperative interactions between adenovirus vectors expressing bone morphogenetic proteins 2, 4, and 7. *J Cell Biochem* **95**: 1–16.
18. Riew, KD, Wright, NM, Cheng, S, Avioli, LV and Lou, J (1998). Induction of bone formation using a recombinant adenoviral vector carrying the human BMP-2 gene in a rabbit spinal fusion model. *Calcif Tissue Int* **63**: 357–360.
19. Rutherford, RB, Moalli, M, Franceschi, RT, Wang, D, Gu, K and Krebsbach, PH (2002). Bone morphogenetic protein-transduced human fibroblasts convert to osteoblasts and form bone *in vivo*. *Tissue Eng* **8**: 441–452.
20. Schek, RM, Hollister, SJ and Krebsbach, PH (2004). Delivery and protection of adenoviruses using biocompatible hydrogels for localized gene therapy. *Mol Ther* **9**, 130–138.
21. Gafni, Y, Pelled, G, Zilberman, Y, Turgeman, G, Apparailly, F, Yotvat, H *et al.* (2004). Gene therapy platform for bone regeneration using an exogenously regulated, AAV-2-based gene expression system. *Mol Ther* **9**: 587–595.
22. Lundstrom, K (2003). Latest development in viral vectors for gene therapy. *Trends Biotechnol* **21**: 117–122.
23. Egermann, M, Lill, CA, Griesbeck, K, Evans, CH, Robbins, PD, Schneider, E *et al.* (2006). Effect of BMP-2 gene transfer on bone healing in sheep. *Gene Ther* **13**: 1290–1299.
24. Kanayama, N, Fukushima, S, Nishiyama, N, Itaka, K, Jang, WD, Miyata, K *et al.* (2006). A PEG-based biocompatible block catiomer with high buffering capacity for the construction of polyplex micelles showing efficient gene transfer toward primary cells. *ChemMedChem* **1**: 439–444.
25. Harada-Shiba, M, Yamauchi, K, Harada, A, Takamisawa, I, Shimokado, K and Kataoka, K (2002). Polyion complex micelles as vectors in gene therapy—pharmacokinetics and *in vivo* gene transfer. *Gene Ther* **9**: 407–414.
26. Itaka, K, Harada, A, Nakamura, K, Kawaguchi, H and Kataoka, K (2002). Evaluation by fluorescence resonance energy transfer of the stability of nonviral gene delivery vectors under physiological conditions. *Biomacromolecules* **3**: 841–845.
27. Itaka, K, Yamauchi, K, Harada, A, Nakamura, K, Kawaguchi, H and Kataoka, K (2003). Polyion complex micelles from plasmid DNA and poly(ethylene glycol)-poly(L-lysine) block copolymer as serum-tolerable polyplex system: physicochemical properties of micelles relevant to gene transfection efficiency. *Biomaterials* **24**: 4495–4506.
28. Boussif, O, Lezoualc'h, F, Zanta, MA, Mergny, MD, Scherman, D, Demeneix, B *et al.* (1995). A versatile vector for gene and oligonucleotide transfer into cells in culture and *in vivo*: polyethylenimine. *Proc Natl Acad Sci USA* **92**: 7297–7301.
29. Hellgren, I, Drvota, V, Pieper, R, Enoksson, S, Blomberg, P, Islam, KB *et al.* (2000). Highly efficient cell-mediated gene transfer using non-viral vectors and FuGene6: *in vitro* and *in vivo* studies. *Cell Mol Life Sci* **57**: 1326–1333.
30. Weiskirchen, R, Kneifel, J, Weiskirchen, S, van de Leur, E, Kunz, D and Gressner, AM (2000). Comparative evaluation of gene delivery devices in primary cultures of rat hepatic stellate cells and rat myofibroblasts. *BMC Cell Biol* **1**: 4.
31. Lee, MJ, Cho, SS, You, JR, Lee, Y, Kang, BD, Choi, JS *et al.* (2002). Intraperitoneal gene delivery mediated by a novel cationic liposome in a peritoneal disseminated ovarian cancer model. *Gene Ther* **9**: 859–866.
32. Elmadbouh, I, Rossignol, P, Meilhac, O, Vranckx, R, Pichon, C, Pouzet, B *et al.* (2004). Optimization of *in vitro* vascular cell transfection with non-viral vectors for *in vivo* applications. *J Gene Med* **6**: 1112–1124.
33. Tinsley, RB, Faijerson, J and Eriksson, PS (2006). Efficient non-viral transfection of adult neural stem/progenitor cells, without affecting viability, proliferation or differentiation. *J Gene Med* **8**: 72–81.
34. Ohba, S, Ikeda, T, Kugimiya, F, Yano, F, Lichtler, AC, Nakamura, K *et al.* (2007). Identification of a potent combination of osteogenic genes for bone

regeneration using embryonic stem (ES) cell-based sensor. *FASEB J* (epub ahead of print).
35. Hunter, AC (2006). Molecular hurdles in polyfectin design and mechanistic background to polycation induced cytotoxicity. *Adv Drug Deliv Rev* **58**: 1523–1531.
36. Bonadio, J, Smiley, E, Patil, P and Goldstein, S (1999). Localized, direct plasmid gene delivery *in vivo*: prolonged therapy results in reproducible tissue regeneration. *Nat Med* **5**: 753–759.
37. Verma, IM and Somia, N (1997). Gene therapy—promises, problems and prospects. *Nature* **389**: 239–242.
38. Bright, C, Park, YS, Sieber, AN, Kostuik, JP and Leong, KW (2006). *In vivo* evaluation of plasmid DNA encoding OP-1 protein for spine fusion. *Spine* **31**: 2163–2172.
39. Huang, YC, Simmons, C, Kaigler, D, Rice, KG and Mooney, DJ (2005). Bone regeneration in a rat cranial defect with delivery of PEI-condensed plasmid DNA encoding for bone morphogenetic protein-4 (BMP-4). *Gene Ther* **12**: 418–426.
40. Moghimi, SM, Symonds, P, Murray, JC, Hunter, AC, Debska, G and Szewczyk, A (2005). A two-stage poly(ethylenimine)-mediated cytotoxicity: implications for gene transfer/therapy. *Mol Ther* **11**: 990–995.
41. Geiger, F, Bertram, H, Berger, I, Lorenz, H, Wall, O, Eckhardt, C *et al.* (2005). Vascular endothelial growth factor gene-activated matrix (VEGF165-GAM) enhances osteogenesis and angiogenesis in large segmental bone defects. *J Bone Miner Res* **20**: 2028–2035.
42. Omidi, Y, Hollins, AJ, Benboubetra, M, Drayton, R, Benter, IF and Akhtar, S (2003). Toxicogenomics of non-viral vectors for gene therapy: a microarray study of lipofectin- and oligofectamine-induced gene expression changes in human epithelial cells. *J Drug Target* **11**: 311–323.
43. Kabanov, AV, Batrakova, EV, Sriadibhatla, S, Yang, Z, Kelly, DL and Alakov, VY (2005). Polymer genomics: shifting the gene and drug delivery paradigms. *J Control Release* **101**: 259–271.
44 Buttery, LD, Bourne, S, Xynos, JD, Wood, H, Hughes, FJ, Hughes, SP *et al.* (2001). Differentiation of osteoblasts and *in vitro* bone formation from murine embryonic stem cells. *Tissue Eng* **7**: 89–99.
45. Jiang, Y, Vaessen, B, Lenvik, T, Blackstad, M, Reyes, M and Verfaillie, CM (2002). Multipotent progenitor cells can be isolated from postnatal murine bone marrow, muscle, and brain. *Exp Hematol* **30**: 896–904.
46. Seto, H, Kamekura, S, Miura, T, Yamamoto, A, Chikuda, H, Ogata, T *et al.* (2004). Distinct roles of Smad pathways and p38 pathways in cartilage-specific gene expression in synovial fibroblasts. *J Clin Invest* **113**: 718–726.
47. Hirata, K, Tsukazaki, T, Kadowaki, A, Furukawa, K, Shibata, Y, Moriishi, T *et al.* (2003). Transplantation of skin fibroblasts expressing BMP-2 promotes bone repair more effectively than those expressing Runx2. *Bone* **32**: 502–512.
48. Cowan, CM, Shi, YY, Aalami, OO, Chou, YF, Mari, C, Thomas, R *et al.* (2004). Adipose-derived adult stromal cells heal critical-size mouse calvarial defects. *Nat Biotechnol* **22**: 560–567.
49. Kugimiya, F, Kawaguchi, H, Kamekura, S, Chikuda, H, Ohba, S, Yano, F *et al.* (2005). Involvement of endogenous bone morphogenetic protein (BMP) 2 and BMP6 in bone formation. *J Biol Chem* **280**: 35704–35712.

Gene Therapy (2007) 14, 1029–1038

www.nature.com/gt

**ORIGINAL ARTICLE**

# Biocompatible micellar nanovectors achieve efficient gene transfer to vascular lesions without cytotoxicity and thrombus formation

D Akagi[1,2], M Oba[3], H Koyama[3], N Nishiyama[4], S Fukushima[2], T Miyata[1], H Nagawa[1] and K Kataoka[2,4,5]

[1]*Division of Vascular Surgery, Department of Surgery, Graduate School of Medicine, The University of Tokyo, Bunkyo-ku, Tokyo, Japan;* [2]*Department of Materials Engineering, Graduate School of Engineering, The University of Tokyo, Bunkyo-ku, Tokyo, Japan;* [3]*Department of Vascular Regeneration, Graduate School of Medicine, The University of Tokyo, Bunkyo-ku, Tokyo, Japan;* [4]*Division of Clinical Biotechnology, Center for Disease Biology and Integrative Medicine, Graduate School of Medicine, The University of Tokyo, Bunkyo-ku, Tokyo, Japan and* [5]*Center for NanoBio Integration, The University of Tokyo, Bunkyo-ku, Tokyo, Japan*

*Gene therapy, a promising treatment for vascular disease, requires appropriate gene vectors with high gene transfer efficiency, good biocompatibility and low cytotoxicity. To satisfy these requirements from the approach of nonviral vectors, a novel block copolymer, poly(ethylene glycol) (PEG)-block-polycation, carrying ethylenediamine units in the side chain (PEG-b-P[Asp(DET)]) was prepared. PEG-b-P[Asp(DET)] formed a polyplex micelle through polyion complex formation with plasmid DNA (pDNA). The PEG-b-P[Asp(DET)] polyplex micelle showed efficient gene expression with low cytotoxicity against vascular smooth muscle cells* in vitro. *It also showed reduced interactions with blood components, offering its feasibility of gene delivery via the vessel lumen. To evaluate* in vivo *gene transfer efficiency for vascular lesions, PEG-b-P[Asp(DET)] micelle was instilled into rabbit carotid artery with neointima by an intravascular method, and expression of the reporter gene in vascular lesions was assessed. Polyplexes from homopolymer P[Asp(DET)] and branched polyethyleneimine (BPEI) were used as controls. Ultimately, only the polyplex micelle showed appreciable gene transfer into vascular lesions without any vessel occlusion by thrombus, which was in strong contrast to BPEI and P[Asp(DET)] polyplexes which frequently showed occlusion with thrombus. These findings suggest that the PEG-b-P[Asp(DET)] polyplex micelle may have promising potential as a nonviral vector for the treatment of vascular diseases.*
Gene Therapy (2007) **14**, 1029–1038. doi:10.1038/sj.gt.3302945; published online 26 April 2007

**Keywords:** *gene delivery; non-viral gene vector; polyplex micelle; vascular disease; intimal hyperplasia; biocompatibility*

## Introduction

Local gene delivery is a promising approach for the treatment of refractory vascular disease. Previous studies have presented a variety of strategies for transferring therapeutic genes to the vascular wall.[1,2] Viral vectors, such as adenovirus vector, have been commonly utilized in these strategies, because the gene transfer efficiency with a viral vector is generally higher than that by other nonviral methods. However, the clinical use of viral vectors has considerable limitations with respect to safety.[3,4] For therapeutic application of gene delivery to the vascular wall, it is, therefore, desirable to develop a nonviral vector with safety and reasonable efficiency of gene transfer.

Several cationic polymers (polycations), which form a polyion complex with DNA (polyplex) and then promote introduction of the DNA into cells, have been widely used as nonviral vectors in several studies *in vitro*.[5,6] However, positively charged polyplexes might potentially induce cytotoxicity and form aggregates in biological media containing plasma proteins, indicating that *in vivo* applications of such polyplexes might be markedly restricted.[7,8] To resolve this issue, we recently designed biocompatible nonviral vectors constructed from newly synthesized cationic block copolymer.[9] The block copolymer thus synthesized is characterized by tandem alignment of a hydrophilic poly(ethylene glycol) (PEG) segment and a cationic polyaspartamide segment carrying an ethylenediamine unit at the side chain (PEG-*b*-P[Asp(DET)]) (Figure 1a),[10] leading to the formation of stable and biocompatible polyplex micelles with a core of tightly packed plasmid DNA (pDNA) surrounded by a dense shell layer of PEG (Figure 1b). Because of the hydrophilicity as well as the strong steric-repulsive propensity of the PEG shell, the polyplex micelles are assumed to be stable in physiological entities including harsh *in vivo* conditions.[11] Furthermore, after internalization of the polyplex micelles into cellular compartments through the endocytic pathway, the ethylenediamine unit in the block copolymer is expected to facilitate efficient

Correspondence: Professor K Kataoka, Department of Materials Engineering, Graduate School of Engineering, The University of Tokyo, 7-3-1 Hongo, Bunkyo-ku, Tokyo 113-0033, Japan.
E-mail: kataoka@bmw.t.u-tokyo.ac.jp
Received 16 September 2006; revised 24 January 2007; accepted 31 January 2007; published online 26 April 2007

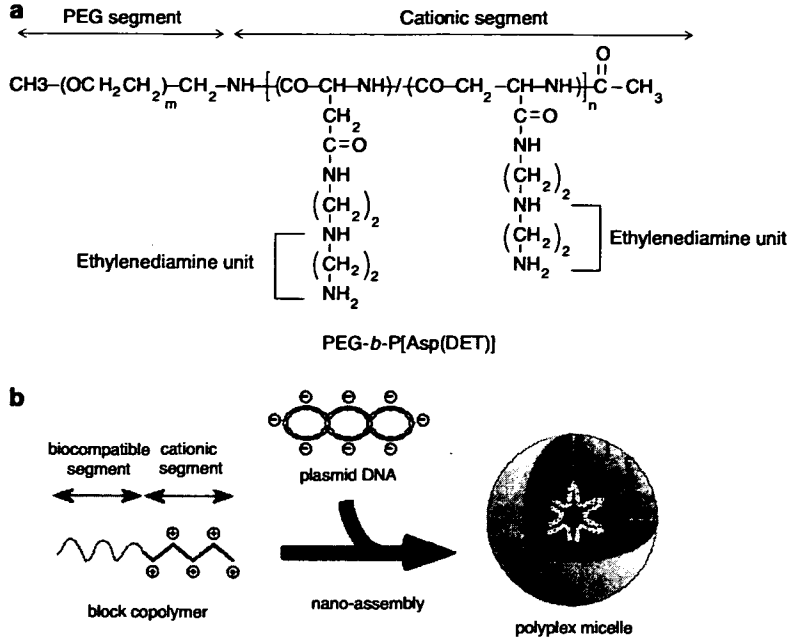


**Figure 1** (a) Chemical structure of PEG-*b*-P[Asp(DET)] block copolymer. (b) Schematic illustrations of the polyplex micelle formation through electrostatic force.

translocation of the micelle toward the cytoplasm due to the proton sponge mechanism based on its high buffering capacity.[12] A previous study indeed revealed that polyplex micelles made from PEG-*b*-P[Asp(DET)] accomplished appreciably high gene transfection efficacy with remarkably low cytotoxicity toward several cultured cell lines as well as primary osteoblasts.[10]

In the present study, the utility of the polyplex micelle from PEG-*b*-P[Asp(DET)] for transfection to vascular lesions was investigated to evaluate its feasibility for vascular gene therapy. The polyplex micelle was revealed to have excellent colloidal stability even in proteinaceous medium and reduced interactions with blood components, showing appreciable gene transfection efficacy toward primary vascular smooth muscle cells (VSMC) under *in vitro* conditions. Furthermore, *in vivo* transfection of a reporter gene to rabbit carotid artery with induced neointimal lesions was successfully done, with high transfection ability and markedly reduced cytotoxicity and thrombogenicity of the polyplex micelles, making it feasible for vascular gene therapy.

## Results

### In vitro *gene transfer to VSMC*

The gene expression efficacy was evaluated as expressed luciferase activity. Expression pDNA containing the luciferase gene (*pCAccluc+*) was transferred to cultured VSMC using the polyplex micelle from PEG-*b*-P[Asp(DET)] to assess the gene transfection efficiency of the micelle from the activity of expressed luciferase after 48 h of culture. Polyplexes from branched polyethyleneimine (BPEI) and P[Asp(DET)] were used as controls. Note that P[Asp(DET)] is the homopolymer of Asp(DET), and was selected as a control to estimate the effect of PEG

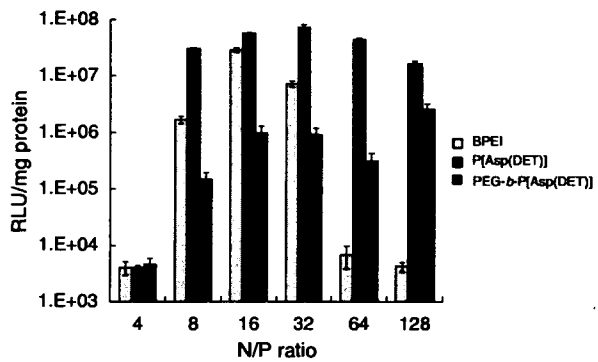


**Figure 2** *In vitro* gene expression as measured by luciferase activity at 48 h after administration of BPEI polyplex, P[Asp(DET)] polyplex and PEG-*b*-P[Asp(DET)] micelle. Each polymer was complexed with pCAcc-luc+ at various N/P ratios, and applied to cultured VSMC. Forty-eight hours later, the cells were lysed, and luciferase activity of the lysates was measured. Values are expressed as RLU/mg protein. Values are shown as mean ± s.e.m.

on physicochemical and biological characteristics of the polyplexes. Polyplexes of BPEI and P[Asp(DET)] as well as polyplex micelles of PEG-*b*-P[Asp(DET)] were prepared by mixing the corresponding polymer with pDNA at various N/P ratios. Here, N/P ratio refers to the unit molar ratio of the amino group in the polymer to the phosphate group in the pDNA. BPEI polyplex showed maximum transfection at an N/P ratio of 16 (Figure 2), followed by a steep decrease in efficacy, presumably due to increased cytotoxicity, as shown in Figure 3. Notably, VSMC transfected with P[Asp(DET)] polyplex and PEG-*b*-P[Asp(DET)] polyplex micelle maintained appreciably high luciferase activity at a wide range of N/P ratios >8, consistent with their lowered cytotoxicity (Figure 3). P[Asp(DET)] polyplex achieved more than tenfold higher

transfection activity than the PEG-*b*-P[Asp(DET)] micelle under this condition, and was even more effective than BPEI polyplex. It should be noted that transfection was not detectable for naked pDNA under the same conditions (data not shown).

### *Cytotoxicity to VSMC*

Cytotoxicity to VSMC of the polyplexes and the polyplex micelles with varying N/P ratios was evaluated by MTT assay after 48 h of incubation. The viability of cells incubated with BPEI polyplex decreased linearly with an increase in N/P ratio, as seen in Figure 3. In contrast, cellular viability remained at more than 70 and 90% even after 48 h incubation with P[Asp(DET)] polyplex and PEG-*b*-P[Asp(DET)] polyplex micelle, respectively, up to an N/P ratio of 64.

### *Aggregate formation in albumin solution*

To assess the colloidal stability of the polyplexes in biological media, they were subjected to measurements of particle size and ζ-potential after incubation for 1 h in phosphate-buffered saline (PBS) containing various concentrations of albumin. The polyplex micelle prepared at N/P = 40 maintained a size of approximately 110 nm regardless of albumin concentration, as summarized in Table 1, yet polyplexes from both BPEI (N/P = 10) and P[Asp(DET)] (N/P = 40) exhibited a marked increase in particle size in medium containing albumin at 1–2 mg/ml. The polyplexes from BPEI and P[Asp(DET)] showed highly positive ζ-potential values (~26 mV) in the absence of albumin, whereas their ζ-potential values decreased toward a neutral value with an increase in albumin concentration, presumably due to the association with anionically charged albumin molecules (Figure 4). This nonspecific association with albumin is likely to be the reason for the aggregate formation of the polyplex system in the presence of albumin observed in Table 1. In contrast, the polyplex micelle had an almost neutral ζ-potential with a small absolute value over a wide range of albumin concentrations (Figure 4), indicating improved colloidal stability of the polyplex micelle compared to conventional polyplexes with a cationic nature.

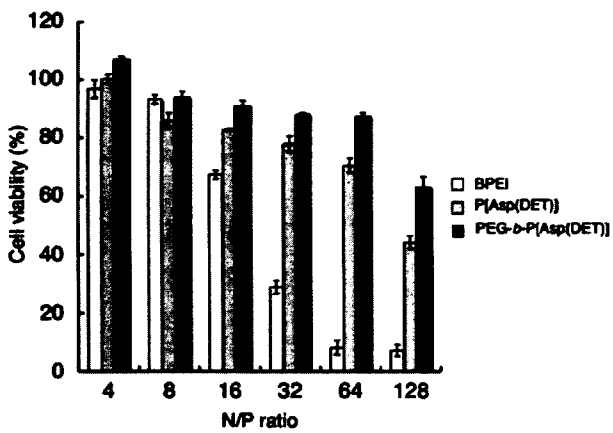


**Figure 3** *In vitro* cytotoxicity to VSMC after 48 h incubation with BPEI polyplex, P[Asp(DET)] polyplex and PEG-*b*-P[Asp(DET)] micelle. Each polymer was complexed with pDNA at various N/P ratios, and applied to cultured VSMC ($n = 4$, each). Forty-eight hours later, cell viability was assessed by MTT assay. Values are shown as mean ± s.e.m.

### *Measurement of platelet aggregation using platelet-rich plasma*

It is known that platelet aggregation plays a pivotal role in the initial stage of the thrombus formation. To estimate the thrombogenicity of the polyplexes and micelles, they were mixed with platelet-rich plasma (PRP), and the platelet aggregation was evaluated by a laser-scattering aggregometer PA-200 (Kowa, Tokyo, Japan). In this measurement, aggregate formation was measured as an increase in the light-scattering intensity (LSI; in mV). The size of detected aggregates was tentatively defined by LSI and was classified as 'small', 'medium' and 'large' as

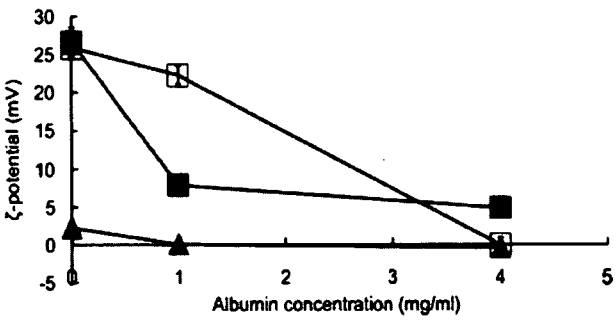


**Figure 4** ζ-potential of BPEI polyplex (N/P = 10) (open squares), P[Asp(DET)] (N/P = 40) (solid squares), and PEG-*b*-P[Asp(DET)] micelle (N/P ratio = 40) (triangles) in the medium containing varying concentrations of albumin solution ($n = 3$). Values are shown as mean ± s.e.m.

**Table 1** Particle size analysis in the medium with varying albumin concentrations (nm)

| | *Albumin concentration (mg/ml)* | | | | | |
|---|---|---|---|---|---|---|
| | *0* | *0.01* | *0.1* | *1* | *2* | *4* |
| BPEI polyplex | 136.3 | 130.0 | 131.3 | 141.7 | ND[a] | ND[a] |
| P[Asp(DET)] polyplex | 141.7 | 120.3 | 167.3 | ND[a] | ND[a] | ND[a] |
| PEG-*b*-P[Asp(DET)] micelle | 112.0 | 108.7 | 117.7 | 111.3 | 112.7 | 111.7 |

Abbreviations: BPEI, branched polyethyleneimine; ND, not determined; PEG, poly(ethylene glycol).
BPEI N/P = 10, P[Asp(DET)] N/P = 40, PEG-*b*-P[Asp(DET)] N/P = 40.
[a]Not determined because of aggregate formation.

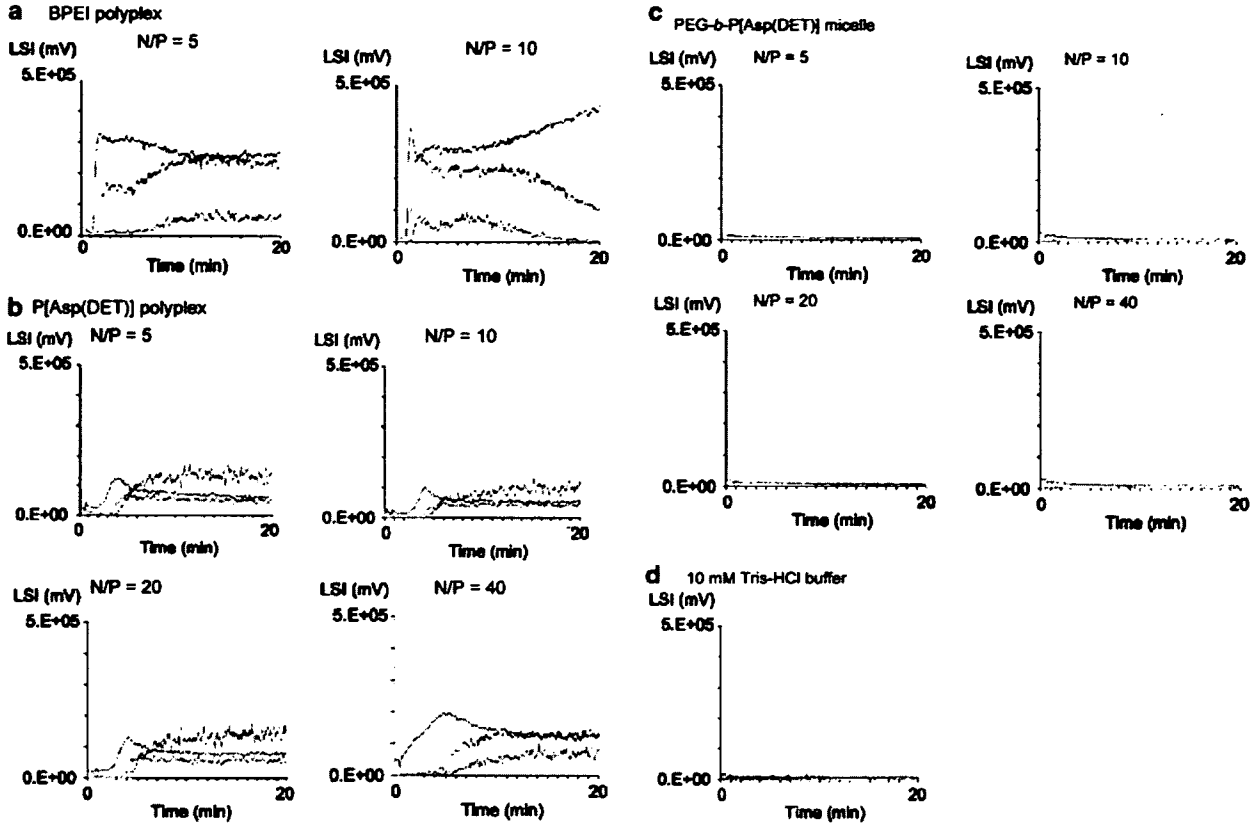


Figure 5 Time-dependent profiles of platelet aggregation by a laser-scattering aggregometer PA-200 after mixing PRP (240 $\mu$l) with the polyplexes (60 $\mu$l) or the micelles (60 $\mu$l); (a) BPEI polyplexes (N/P = 5, 10); (b) P[Asp(DET) polyplexes (N/P = 5, 10, 20, 40); (c) PEG-*b*-P[Asp(DET)] micelle (N/P = 5, 10, 20, 40) and (d) 10 mM Tris-HCl buffer (pH 7.4). The vertical values are expressed as the LSI, the unit of which is milli volts (mV). In each figure, the blue, green and red profiles correspond to the aggregates classified as 'small', 'medium' and 'large' (see Materials and methods section), respectively (Min, minute).

described in the Materials and methods section. BPEI and P[Asp(DET)] polyplexes showed an appreciable increase in the LSI of 'small', 'medium' and 'large' category at any N/P ratios (Figure 5a and b), suggesting the significant platelet aggregation. In contrast, PEG-*b*-P[Asp(DET)] micelle showed no increase in the LSI at any N/P ratios (Figure 5c and d), indicating that the PEG shell of the polyplex micelles effectively prevented the aggregation of platelets.

### *Erythrocyte aggregation assay*

To further study the interaction between the polyplexes and blood cells, erythrocyte aggregation assay was carried out. It is known that erythrocytes possess negative surface charge and interact with positively charged nano-particles, resulting in the aggregate formation.[13] Erythrocytes were harvested from blood of rabbit, followed by washing and suspension with Ringer's solution to avoid the effect of serum proteins. Figure 6 revealed that erythrocytes incubated with BPEI (Figure 6a) and P[Asp(DET)] polyplexes (Figure 6b) underwent aggregation regardless of N/P ratios. By contrast, erythrocytes incubated with PEG-*b*-P[Asp(DET)] micelle did not undergo any aggregation (Figure 6c), keeping the dispersivity comparable to those in 10 mM Tris-HCl buffer (Figure 6d). These results clearly indicate that neutral and sterically repulsive properties of the polyplex micelle might also effectively prevent the erythrocyte aggregation through the electrostatic interaction.

### *Gene transfer to injured rabbit carotid artery*

Rabbit carotid artery was injured with a Fogarty balloon catheter to induce neointimal hyperplasia. Twenty-one days later, BPEI (N/P = 10) polyplex, P[Asp(DET)] (N/P = 40) polyplex, and PEG-*b*-P[Asp(DET)] (N/P = 40) micelle were administered into the carotid artery with neointimal involvement and incubated by cessation of arterial blood flow for 20 min. N/P ratios of the polyplexes and micelles used for *in vivo* experiments were adjusted to the appropriate values based on the results of *in vitro* experiments, that is, the balance between the cytotoxicity (Figure 3) and the transfection efficiency (Figure 2). Note that the aggregation assay using albumin (Table 1 and Figure 4), platelets (Figure 5) and erythrocytes (Figure 6) revealed that PEG-*b*-P[Asp(DET)] micelle had minimal interaction with these biocomponents at any N/P ratios. The entrapped pDNA in the polyplex and the micelle was the expression plasmid vector containing the luciferase gene (*pCAccluc+*). Naked pDNA (*pCAccluc+*) was applied in the same manner as controls. At 3 days after the treatment, the carotid arteries were sampled to assess luciferase activity in each layer of the arterial wall (Figure 7a). All of the rabbits that received naked pDNA ($n = 8$) or the polyplex micelle ($n = 8$) had 100% patency of the carotid artery, whereas considerable

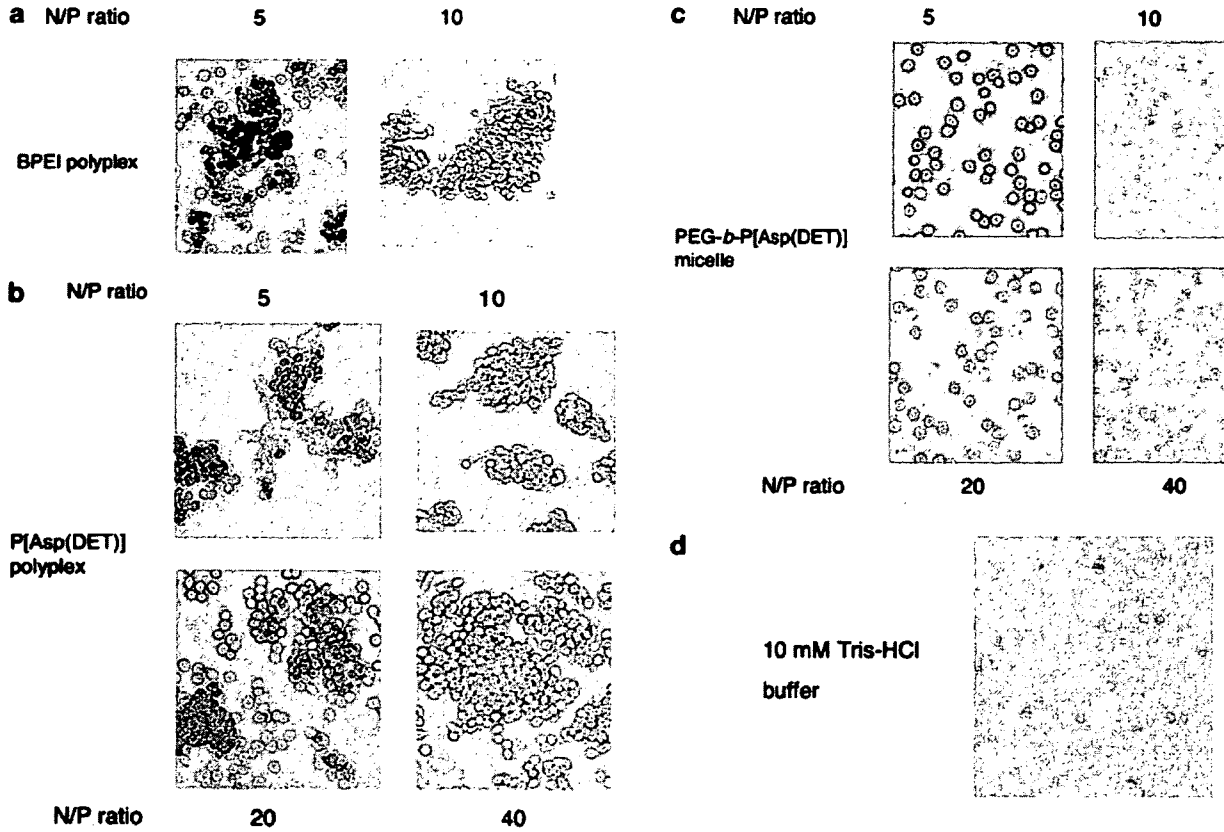


**Figure 6** Photomicrographs of erythrocytes mixed and incubated for 1 h at 37°C with or without polyplexes varying N/P ratios: (**a**) BPEI polyplex (N/P = 5 and 10); (**b**) P[Asp(DET)] polyplex (N/P = 5, 10, 20 and 40); (**c**) PEG-*b*-P[Asp(DET)] micelle (N/P = 5, 10, 20 and 40) and (**d**) control in 10 mM Tris-HCl buffer without any polyplexes (control). Aggregation was observed in the medium containing BPEI and P[Asp(DET)] polyplex regardless of N/P ratios, although no aggregation was observed in the medium with PEG-*b*-P[Asp(DET)] micelle of varying N/P ratio.

thrombo-occlusion of the artery occurred in rabbits in which BPEI (3 occlusions in 8 samples) and P[Asp(DET)] (4 occlusions in 8 samples) polyplexes were applied. The cross sections of the patent and occluded arteries with hematoxylin-eosin stain were shown in Figure 7b–f. The lumens of the occluded arteries challenged with P[Asp(DET)] and BPEI polyplexes were filled with thrombus. All the samples subjected to BPEI polyplex, P[Asp(DET)] polyplex, and PEG-*b*-P[Asp(DET)] polyplex micelles showed significantly higher luciferase activity in the neointima, media and adventitia than those with naked pDNA. There was no significant difference in the luciferase activity among the samples with BPEI, P[Asp(DET)] and PEG-*b*-P[Asp(DET)] treatment (Figure 7a).

To confirm *in vivo* gene transfer to the arterial wall, the expression pDNA containing the FLAG sequence (*pMP-FLAG*) was then complexed with PEG-*b*-P[Asp(DET)] and administered to the carotid artery in the same manner. The artery was harvested on day 3, and a cross section of the artery was stained with anti-FLAG antibody. The immunostain clearly showed abundant FLAG-positive cells in the arterial wall, in which FLAG expression was predominantly observed in the neointima (Figure 8a). The pDNA expressing LacZ gene (*pCAZ3*) was then complexed with PEG-*b*-P[Asp(DET)] and administered to the carotid artery in the same manner as negative control. Eventually, the immunostain with anti-FLAG antibody showed no FLAG-positive cells (Figure 8b) in the control specimen.

## Discussion

Vascular lesions as feasible targets for gene therapy are generally related to atherosclerosis or its associated diseases. As such lesions develop from the intimal layer of the vascular wall, the intima is a primary target of vascular gene therapy, indicating that delivery via the vessel lumen is the most appropriate approach for efficient gene transfer to vascular lesions. Fortunately, it is easy to approach the luminal surface using a catheter-based method, and several endovascular devices have been developed for this purpose in previous studies. In the vessel lumen, however, attention must be paid to interactions between the gene vector and blood components such as plasma proteins and blood cells. In particular, platelet activation and aggregation promote the coagulant and fibrinolytic pathways through activation of coagulation factors accompanying aggregation of blood cells, resulting in thrombus formation. Most nonviral gene vectors possess a positively charged component in their structure to form a complex with DNA. As blood components ordinarily carry a negative

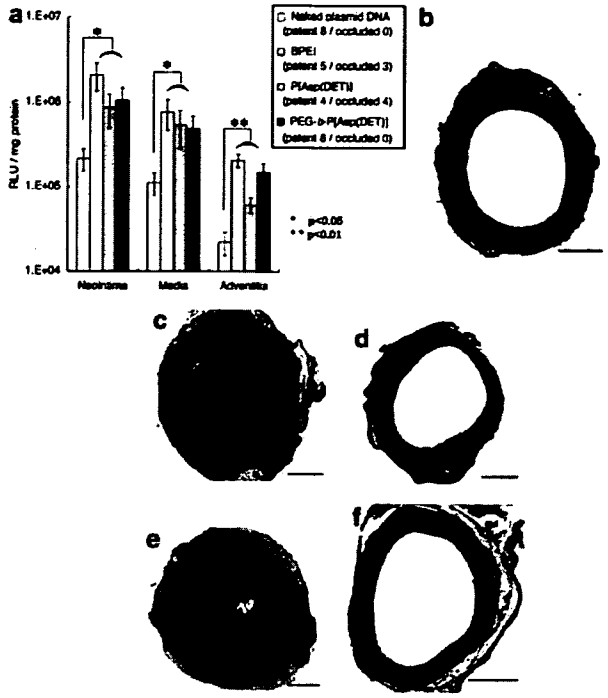


**Figure 7** (a) *In vivo* gene expression evaluated from luciferase activity after intra-arterial delivery of BPEI polyplex (N/P = 10), P[Asp(DET)] polyplex (N/P = 40), and PEG-*b*-P[Asp(DET)] micelle (N/P = 40). Each polymer was complexed with *pCAccluc+* and instilled into the rabbit common carotid artery with neointima. One group of animals was treated with naked pDNA (*pCAccluc+*) as control. At 72 h, the common carotid artery was excised and luciferase activity was measured. Values are expressed as RLU/mg protein. Values are shown as mean ± s.e.m. (*$P<0.01$, **$P<0.05$). (b–f) Cross sections of the gene-transferred arteries with hematoxylin-eosin stain, (b) patent, (c) occluded samples of BPEI polyplexes (N/P = 10), (d) patent, (e) occluded samples of P[Asp(DET)] polyplexes (N/P = 40) and (f) patent sample of PEG-*b*-P[Asp(DET)] micelle (N/P = 40). Bar = 500 μm.

charge, there is a possibility for a nonviral vector to undergo aggregation with plasma proteins and blood cells.[5,13–16] Such aggregation around a gene vector might interfere with the process of gene transfer and also induce thrombus formation, which could worsen the clinical status of the primary disease. Additionally, the positive charge of the gene vector would potentially promote cytotoxic reactions in the lesion and its surrounding part of the vascular wall. As the intima is the most accessible part in vascular gene therapy, as described, the toxic side effects derived from constituent polycations of polyplexes also predominantly appear in the intimal layer of the arterial wall, which might imply injury of intimal cells. In previous studies investigating the mechanisms of atherogenesis, various evidence has been presented to demonstrate that vascular injury is a potent trigger for lesion formation.[17,18] Injury to the vascular wall possibly promotes a variety of responses, such as expression of adhesive molecules and receptors on vascular cells, release of several growth factors, platelet adhesion on the luminal surface and infiltration of inflammatory cells.[19] These responses might influence each other, and potentially induce the formation of neointimal hyperplasia and atherosclerotic lesions. Thus,

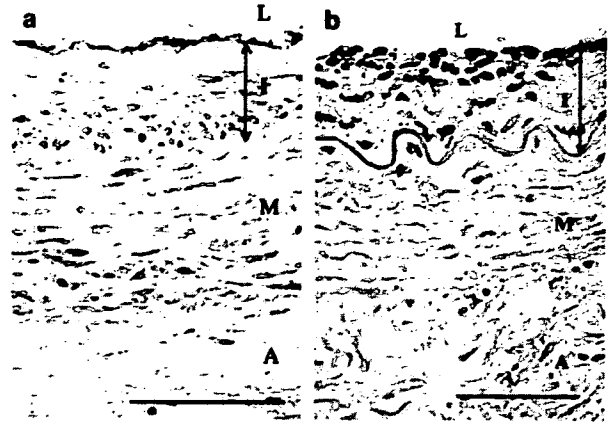


**Figure 8** (a) Photomicrographs of rabbit carotid artery transfected with the polyplex micelle composed of pMP-FLAG and PEG-*b*-P[Asp(DET)] (N/P = 40). (b) Photomicrographs of rabbit carotid artery transfected with the polyplex micelle composed of pDNA expressing LacZ and PEG-*b*-P[Asp(DET)] (N/P = 40) as control. FLAG-positive region was stained brown. L, lumen; I, intima; M, media; A, adventitia. Bar = 100 μm.

minimal vascular injury with biocompatible gene vector systems with low cytotoxicity should be achieved for safe and reliable gene therapy in vascular diseases.

To achieve successful gene delivery to the carotid artery by intravascular method, polyplex micelles, in which the polyplex core is covered with PEG palisades, were used in this study. One of the advantageous characteristics of polyplex micelles with a PEG shell layer is high colloidal stability in a physiological proteinaceous medium, showing reduced interactions with blood components. It was reported that the thrombus formation are caused by nonspecific interaction between blood components and cationic materials such as polyplexes and prosthesis for intravascular application.[13–16,20–24] Srinivasan *et al.*[20] reported that positively charged prosthetic materials are highly thrombogenic. PEG is the well-known materials with hydrophilic character showing the high biocompatibility and the low thrombogenicity.[25–27] There are previous reports that the surface modification of biomaterials with PEG appreciably reduces thrombogenicity.[25,28–32] Thus, it is widely accepted that PEG shields the cationic surface of biomaterials, reducing their thrombogenicity.[31] In this study, the PEG-*b*-P[Asp(DET)] micelle system showed no agglomeration even in the presence of blood components including serum albumin (Table 1 and Figure 4), platelets (Figure 5) and erythrocytes (Figure 6), whereas BPEI and P[Asp(DET)] polyplexes definitely showed the aggregate formation due to their positively charged character under the same conditions. It should be noted that PEG-*b*-P[Asp(DET)] micelle showed no platelet and erythrocyte aggregation even at a high N/P ratios, whereas P[Asp(DET)] and BPEI polyplexes induced platelet and erythrocyte aggregation even at low N/P ratios, such as 5. These results suggest that the surface modification of polyplexes with PEG might prevent their interaction with blood components even at a high N/P ratio required for the effective gene transfection. In addition to the colloidal stability of nonviral vectors with reduced interactions with blood components, another critical issue is the incidence of cytotoxic reactions.

In this regard, the lower cytotoxicity of PEG-*b*-P[Asp(DET)] as compared to BPEI against VSMC, a primary target of vascular gene therapy of atherosclerosis, was demonstrated in Figure 3. Such reduced nonspecific interactions with blood components and low cytotoxicity of polyplex micelles should be the remarkable advantages as the system utilized for *in vivo* nonviral gene delivery via the vascular lumen. Indeed, an *in vivo* study using rabbit carotid artery revealed no occlusion after intraluminal delivery of the polyplex micelle made from PEG-*b*-P[Asp(DET)], whereas the use of polyplexes from BPEI and P[Asp(DET)] resulted in the considerable thrombo-occlusion (Figure 7).

The efficiency of *in vivo* gene transfer is the most important issue in the development of gene vectors for vascular diseases, and the choice of experimental model is crucial for obtaining proper evidence of vascular gene transfer. Experimental studies commonly employ small mammals as animal models, and the artery of such small animals preserves its normal structure even in the adult. In these arteries, because the intima consists of an endothelial monolayer, gene vectors might mainly distribute to the endothelium and medial SMC after administration via the vessel lumen. However, the intimal lesion is the principal target in most vascular gene therapy, and the major cell components of the lesion are intimal SMC and macrophages.[33] Previous studies using an arterial injury model have demonstrated several biological differences between medial SMC and intimal SMC.[33] Also in gene delivery, Guzman *et al.*[34] showed that adenovirus-mediated gene transfer to intimal SMC was highly efficient as compared with that to medial SMC. These findings suggest that the evaluation of vascular gene transfer must be carried out on diseased artery, not normal artery. In the present study, we first induced neointimal hyperplasia in the rabbit carotid artery, and then applied gene vectors to the same artery, which mimicked vascular gene delivery in the clinical setting. Because of the proper preparation of the model, it is expected to provide highly reliable data. In this study, the evaluation using this model showed that gene delivery with the BPEI, P[Asp(DET)], and PEG-*b*-P[Asp(DET)] systems all promoted marked expression of the transferred gene in the neointima, media and adventitia, which was significantly greater than that after the treatment with naked pDNA. In these findings, an interesting feature is that the *in vivo* gene expression level after PEG-*b*-P[Asp(DET)] micelle treatment was similar to that after BPEI or P[Asp(DET)] polyplex treatment (Figure 7a), although the *in vitro* transfection efficiency of the PEG-*b*-P[Asp(DET)] micelle was lower than that of BPEI and P[Asp(DET)] polyplexes (Figure 2). Histological analyses also revealed abundant expression of the marker gene in the arterial wall treated with PEG-*b*-P[Asp(DET)] micelle (Figure 8a), supporting high *in vivo* transfection ability of PEG-*b*-P[Asp(DET)] micelle to vascular lesions. The most likely explanation for such efficient gene transfer to vascular lesions *in vivo* might be an effective buffering action of PEG-*b*-P[Asp(DET)] in the acidic endosomal compartment as described previously.[10]

In conclusion, polyplex micelles from PEG-*b*-P[Asp(DET)] showed excellent colloidal stability with reduced nonspecific interactions with blood components and had a unique feature of the lowered *in vitro* cytotoxicity compared to the conventional polyplexes prepared from BPEI. They achieved efficient gene transfer to the rabbit carotid artery with neointimal hyperplasia without any vascular occlusion, whereas intraluminal delivery of BPEI and P[Asp(DET)] polyplexes induced thrombus formation. Note that the polymerization degree of the polycation segment in the block copolymer is one of the determining factors for the physicochemical property of the polyplex micelles. Block copolymers with relatively shorter polycation segments are not able to form stable polypexes,[35] whereas an increase in the polymerization degree of the polycation segment results in the decreased density of PEG palisades to impair the shielding effect. In this regard, P[Asp(DET)] segment with the polymerization degree of 68 was adopted in this study to construct the block copolymer used in the polyplex micelles, balancing the core stability mainly controlled by the polycation length and the high dispersivity in biological entity correlating mainly with the density of PEG palisades. Eventually, nonspecific interactions with blood components (Table 1, Figures 5 and 6) were effectively shielded, preventing thrombus formation, although achieving appreciable gene transfection, after the intravascular administration (Figure 7). Although there is still an issue of tuning the length of both PEG and P[Asp(DET)] segments in the block copolymer to further optimize the gene transfection and blood compatibility, the concept of the polyplex micelles with the polycation core of low toxicity and high buffering capacity surrounded by the dense PEG palisade was demonstrated to be feasible as nonviral gene vectors useful in the vascular gene therapy.

## Materials and methods

### *Synthesis of block copolymer and homopolymer*

The PEG-*b*-P[Asp(DET)] block copolymer (PEG; Mw = 12 000 g/mol, polymerization degree of P[Asp(DET)]; 68) was prepared as described previously.[10] P[Asp(DET)] was synthesized from poly(*β*-benzyl L-aspartate) (PBLA) by modifying the synthetic method of PEG-P[Asp(DET)]. Briefly, *β*-benzyl-L-aspartate *N*-carboxyanhydride was polymerized in *N,N*-dimethylformamide (DMF)/dichloromethane (1:10) at 40°C by initiation from the primary amino group of *n*-butylamine, followed by acetylation of the *N* terminus to obtain PBLA. A unimodal molecular weight distribution (*Mw/Mn* 1.20) of PBLA was confirmed by gel permeation chromatography (columns: TSK-gel G4000HHR+G3000HHR, eluent: DMF+10 mM LiCl, $T = 40$°C, detector: refractive index). The degree of polymerization of PBLA was calculated as 98 from the $^1$H NMR spectrum (data not shown). Then, the side-chain aminolysis reaction of PBLA was performed by mixing with a 50-fold excess of diethylenetriamine in DMF at 40°C to obtain P[Asp(DET)]. DMF, dichloromethane, and acetic anhydride were purchased from Wako Pure Chemical Industries (Osaka, Japan).

### *Plasmids*

Plasmid *pCAccluc+* was constructed by inserting the recombinant luciferase gene (luc+) into the pCAGGS expression vector. *pCAccluc+* was utilized for all experiments in the present study except morphological

evaluation. Meanwhile, plasmid *pME-FLAG* was constructed by inserting the FLAG tag sequence into the pME expression vector, and used for morphological assessment by immunohistochemical staining. Plasmid *pCAZ3* was constructed by inserting *Escherichia coli* LacZ cDNA into the pCGGGS expression vector. Plasmids were grown in *E. coli* JM109 and purified using Qiagen EndoFree Mega Kits (Qiagen, Hilden, Germany). pDNA was dissolved separately in 10 mM Tris-HCl buffer (pH 7.4), to be 375 $\mu$g/ml.

### *Preparation of polyplex micelle and other polyplexes*

Given amounts of PEG-*b*-P[Asp(DET)], P[Asp(DET)] and BPEI were dissolved in Tris-HCl buffer (10 mM, pH 7.40) separately. The concentrations of polymers, PEG-*b*-P[Asp(DET)], P[Asp(DET)] and BPEI were 40, 20 and 5 mg/ml respectively. The polymer solution of PEG-*b*-P[Asp(DET)] was added at varying concentrations and mixed to a 2-fold excess volume of pDNA solution to form polyplex micelles at various N/P ratios. Polyplex micelles were kept overnight before being subjected to evaluation. Polymer with P[Asp(DET)] or BPEI (Mw = 25 kD, Sigma Chemical, MO, USA) was also mixed with pDNA at various N/P ratios to form polyplex. Each polyplex was subjected to evaluation 30 min after mixing.

### In vitro *gene transfer to VSMC*

Human VSMC (Applied Cell Biology Research Institute, WA, USA) were seeded on 24-well culture plates and cultured in 500 $\mu$l CS-C medium (Applied Cell Biology) containing 10% serum. When the cells were in a semi-confluent condition, a solution of polyplexes (BPEI and P[Asp(DET)]) or polyplex micelle (PEG-*b*-P[Asp(DET)]) was added to each well (1 $\mu$g pDNA/well) ($n = 4$, each). After 24 h of incubation, the cells were washed with PBS and incubated additionally in CS-C for 24 h. N/P ratios of the polyplexes and the micelle were adjusted to 4, 8, 16, 32, 64 and 128. The cells were lysed in 100 $\mu$l cell culture lysis reagent (Promega, WI, USA), and luciferase activity of each lysate was quantified using a Luciferase Assay Kit (Promega). The results were expressed as relative light units (RLU) per milligram of total protein measured by bicinchoninic acid assay (Pierce, IL, USA). The experiment was repeated three times.

### *Cytotoxicity to VSMC*

VSMC were seeded into 96-well plates and cultured in 100 $\mu$l CS-C. When the cells reached a semi-confluent condition, the polyplexes (BPEI and P[Asp(DET)]) or the micelle (PEG-*b*-P[Asp(DET)]) at various N/P ratios was added to each well (0.25 $\mu$g DNA/well) ($n = 4$, each). After 24 h of incubation, the cells were washed, and cultured in CS-C for an additional 24 h. Subsequently, cell viability in each well was evaluated using MTT assay reagent (Dojindo, Kumamoto, Japan) according to manufacturer's instructions. The experiment was repeated three times.

### *Dynamic light-scattering and laser-Doppler electrophoresis measurements*

In dynamic light-scattering (DLS) measurement, the polyplexes, BPEI (N/P = 10) and P[Asp(DET)] (N/P = 40), or the micelle, PEG-*b*-P[Asp(DET)] (N/P = 40), were diluted in 10 mM Tris-HCl buffer (pH 7.4) to adjust the concentration of pDNA to 33.3 $\mu$g/ml ($n = 3$, each). DLS measurement was then carried out at 25 ± 0.2°C using a Zetasizer Nano ZEN3600 (Malvern Instruments, Worcestershire, UK) with a vertically polarized incident beam of 488 nm from an Ar ion laser. The scattering angle was fixed at 173°. The data were analyzed by a cumulative method to obtain the hydrodynamic diameter.

Laser-Doppler electrophoresis measurements were performed at 25 ± 0.2°C using a Zetasizer Nano equipped with a He–Ne ion laser (633 nm), and the scattering angle was set at 17° ($n = 3$, each). From the electrophoretic mobility ($\eta$), the $\zeta$-potential was calculated using the Smoluchowski equation as follows: $\zeta = 4\pi\eta\upsilon/\varepsilon$, where $\upsilon$ is the viscosity and $\varepsilon$ the dielectric constant of the solvent. The experiment was performed twice.

### *Measurement of platelet aggregation*

Fresh blood from Japanese white rabbits (weight, 2.5–3.0 kg; Saitama Rabbitary, Saitama, Japan) was collected and immediately mixed with a 1:9 volume of 3.8% sodium citrate solution. PRP was isolated by centrifugation at the speed of 900 rounds per minute for 11 min at room temperature and collected as the supernatant. BPEI polyplexes (N/P = 5, 10), P[Asp(DET)] polyplexes (N/P = 5, 10, 20 and 40) and PEG-*b*-P[Asp(DET)] micelles (N/P = 5, 10, 20 and 40) were diluted in 10 mM Tris-HCl buffer (pH 7.4) to adjust the concentration of pDNA to 200 $\mu$g/ml. As a negative control, PRP in 10 mM Tris-HCl buffer (pH 7.4) without polyplexes were also used.

Aggregation of platelets in PRP with polyplexes or micelles was evaluated by a laser-scattering aggregometer PA-200 (Kowa). This instrument was reported to sensitively detect small aggregates consisting of only dozens of platelets formed under weak agonists.[36–39] The LSI was measured with the PA-200 to evaluate the existence and the extent of aggregates. According to the default configuration of the PA-200, the LSI was categorized to 'small', 'medium' and 'large' corresponding, respectively, to the small aggregates (9–25 $\mu$m), medium aggregates (26–50 $\mu$m) and large aggregates (51–70 $\mu$m). The results were recorded on a two-dimensional graph showing the time-dependent changes in the LSI. These experiments were repeated three times, and the representative data were shown as the results.

### *Erythrocyte aggregation assay*

Fresh blood from Japanese white rabbits (weight, 2.5–3.0 kg; Saitama Rabbitary) was collected and immediately mixed with 20 $\mu$l heparin sodium. Erythrocytes were washed three times and suspended in Ringer's solution. Washed erythrocyte suspension (800 $\mu$l) was mixed with polyplex solution (400 $\mu$l) and incubated for 1 h at 37°C. BPEI polyplexes (N/P = 5 and 10), P[Asp(DET)] polyplexes (N/P = 5, 10, 20 and 40) and PEG-*b*-P[Asp(DET)] micelles (N/P = 5, 10, 20 and 40) were subjected to the measurement. They were all diluted in 10 mM Tris-HCl buffer (pH 7.4) to adjust the concentration of pDNA to 200 $\mu$g/ml. As a negative control, erythrocytes in 10 mM Tris-HCl buffer (pH 7.4) without polyplexes were also prepared. Aggregation of erythrocytes was evaluated under the optical microscope (Olympus, Tokyo, Japan).

### *Animal model and evaluation of gene transfer efficiency*

All animal experiments conformed to the Guide for Care and Use of Laboratory Animals by the US National Institutes of Health (NIH Publication No. 85–23, revised 1996). Japanese white rabbits (weight, 2.5–3.0 kg; Saitama Rabbitary) fed a normal diet were anesthetized by intramuscular injection of xylazine (2.5 mg/kg) and ketamine (50 mg/kg). A 2 Fr Fogarty balloon catheter (Baxter Healthcare, CA, USA) was introduced through the first branch of the left external carotid artery and passed into the left common carotid artery. The balloon was inflated at physiological pressure and passed through the common carotid artery three times with constant rotation. At 21 days after balloon injury, proximal sites of the common carotid artery and internal carotid artery were clamped, and the left common carotid artery was filled with the polyplexes, BPEI (N/P = 10) and P[Asp(DET)] (N/P = 40), or the micelle, PEG-*b*-P[Asp(DET)] (N/P = 40), through the external carotid artery. In all experiments, each common carotid artery received 400 $\mu$l pDNA containing solution (200 $\mu$g/ml, 80 $\mu$g pDNA). After 20 min incubation, the vector solution was flushed out for washing, and then the arterial circulation was restored. As control, one group of rabbits was treated with naked pDNA (80 $\mu$g pCAccluc+) solution in the same manner. Three days later, animals were sacrificed. Evans blue (1 ml of 5% solution) was injected intravenously to mark the neointimal layer of the artery 10 min before sacrificing the animals. Then the left common carotid artery was excised and the connective tissue around the excised artery was removed, and the artery was opened longitudinally. Under a stereomicroscope, blue-stained neointima was first isolated from the artery, and then the elastic medial layer was separated from the adventitia. Each obtained sample was homogenized and lysed in 200 $\mu$l cell culture lysis reagent, and luciferase activity of each lysate was measured as described. Gene transfer efficiency was presented as the ratio of luciferase activity to the protein content. The results were expressed as RLU/mgtotal protein.

### *Immunohistochemical study*

To evaluate the distribution of gene expression after gene transfer with PEG-*b*-P[Asp(DET)] micelles, pME-FLAG was complexed with PEG-*b*-P[Asp(DET)] (N/P = 40) and applied to rabbit carotid artery in the same manner. Three days after gene delivery, rabbits were sacrificed and subjected to perfusion fixation with 4% phosphate buffered paraformaldehyde (0.1 mol/l $PO_4$ buffer, pH 7.3). The carotid arteries were excised and embedded in paraffin. Cross sections (4 $\mu$m) were immunostained with a monoclonal antibody against FLAG tag (1:100, Sigma), as described previously. As a negative control, the cross sections, where PEG-*b*-P[Asp(DET)] (N/P = 40) micelle with LacZ gene (pCAZ3) was instilled, were stained with anti-FLAG tag antibody.

### *Statistical analysis*

All values are shown as mean $\pm$ s.e.m. of biological experiments. The data of *in vivo* luciferase activity were shown as RLU/mg protein, analyzed by unpaired Student's *t*-test and considered significant at $P < 0.05$.

## Acknowledgements

This work was supported by The Special Coordination Funds for Promoting Science and Technology from the Ministry of Education, Culture, Sports, Science and Technology (MEXT), and the Core Research Program for Evolutional Science and Technology (CREST) from the Japan Science and Technology Corporation (JST). We are especially grateful to Drs Yuichi Yamasaki, Keiji Itaka, Kensuke Osada, Kanjiro Miyata, Mr Satoru Matsumoto and Mr Shunsaku Asano (The University of Tokyo) for their special technical advice. We thank Dr Makoto Kaneko and Professor Yutaka Yatomi (The University of Tokyo) for supporting us at assessing platelet aggregation. And we also thank Mr Noboru Sunaga Ms Junko Kawakita for their assistance.

## References

1 Taniyama Y, Tachibana K, Hiraoka K, Namba T, Yamasaki K, Hashiya N *et al.* Local delivery of plasmid DNA into rat carotid artery using ultrasound. *Circulation* 2002; **105**: 1233–1239.
2 Nishikage S, Koyama H, Miyata T, Ishii S, Hamada H, Shigematsu H. *In vivo* electroporation enhances plasmid-based gene transfer of basic fibroblast growth factor for the treatment of ischemic limb. *J Surg Res* 2004; **120**: 37–46.
3 Edelstein ML, Abedi MR, Wixon J, Edelstein RM. Gene therapy clinical trials worldwide 1989–2004 – an overview. *J Gene Med* 2004; **6**: 597–602.
4 Tomanin R, Scarpa M. Why do we need new gene therapy viral vectors? Characteristics, limitations and future perspectives of viral vector transduction. *Curr Gene Ther* 2004; **4**: 357–372.
5 Wagner E, Ogris M, Zauner W. Polylysine-based transfection systems utilizing receptor-mediated delivery. *Adv Drug Deliv Rev* 1998; **30**: 97–113.
6 Oupicky D, Konak C, Ulbrich K, Wolfert MA, Seymour LW. DNA delivery systems based on complexes of DNA with synthetic polycations and their copolymers. *J Control Release* 2000; **65**: 149–171.
7 Ogris M, Brunner S, Schuller S, Kircheis R, Wagner E. PEGylated DNA/transferrin-PEI complexes: reduced interaction with blood components, extended circulation in blood and potential for systemic gene delivery. *Gene Ther* 1999; **6**: 595–605.
8 Oupicky D, Konak C, Dash PR, Seymour LW, Ulbrich K. Effect of albumin and polyanion on the structure of DNA complexes with polycation containing hydrophilic nonionic block. *Bioconjug Chem* 1999; **10**: 764–772.
9 Katayose S, Kataoka K. Water-soluble polyion complex associates of DNA and poly(ethylene glycol)-poly(L-lysine) block copolymer. *Bioconjug Chem* 1997; **8**: 702–707.
10 Kanayama N, Fukushima S, Nishiyama N, Itaka K, Jang W-D, Miyata K *et al.* A PEG-based biocompatible block catiomer with high buffering capacity for the construction of polyplex micelles showing efficient gene transfer toward primary cells. *ChemMedChem* 2006; **1**: 439–444.
11 Harada-Shiba M, Yamauchi K, Harada A, Takamisawa I, Shimokado K, Kataoka K. Polyion complex micelles as vectors in gene therapy – pharmacokinetics and *in vivo* gene transfer. *Gene Therapy* 2002; **9**: 407–414.
12 Behr JP. The proton sponge. A trick to enter cells the viruses did not exploit. *Chimia* 1999; **51**: 34–36.
13 Kircheis R, Wightman L, Schreiber A, Robitza B, Rossler V, Kursa M *et al.* Polyethyleneimine/DNA complexes shielded by transferrin target gene expression to tumors after systemic application. *Gene Therapy* 2001; **8**: 28–40.

14 Chonn A, Semple S, Cullis P. Association of blood proteins with large unilamellar liposomes *in vivo*. Relation to circulation lifetimes. *J Biol Chem* 1992; **1111**: 239–246.
15 Dash PR, Read ML, Barrett LB, Wolfert MA, Seymour LW. Factors affecting blood clearance and *in vivo* distribution of polyelectrolyte complexes for gene delivery. *Gene Therapy* 1999; **6**: 643–650.
16 Kircheis R, Wagner E. Polycation/DNA complexes for *in vivo* gene delivery. *Gene Therapy Regul* 2000; **1**: 95–114.
17 Koyama H, Olson NE, Dastvan FF, Reidy MA. Cell replication in the arterial wall: activation of signaling pathway following *in vivo* injury. *Circ Res* 1998; **82**: 713–721.
18 Koyama H, Olson NE, Reidy MA. Cell signaling in injured rat arteries. *Thromb Haemost* 1999; **82**: 806–809.
19 Clinton SK, Libby P. Cytokines and growth factors in atherogenesis. *Arch Pathol Lab Med* 1992; **116**: 1292–1300.
20 Srinivasan S, Sawyer PN. Role of surface charge of the blood vessel wall, blood cells, and prosthetic materials in intravascular thrombosis. *J Colloid Interface Sci* 1970; **32**: 456–463.
21 Kataoka K, Akaike T, Sakurai Y, Tsuruta T. Effect of charge and molecular structure of polyion complexes on the morphology of adherent blood platelets. *Makromol Chem* 1978; **179**: 1121–1124.
22 Kataoka K, Tsuruta T, Akaike T, Sakurai Y. Biomedical behavior of synthetic polyion complexes toward blood platelets. *Makromol Chem* 1980; **181**: 1363–1373.
23 Seaman GV. Plasma protein interactions at biological interfaces. *Thromb Res* 1983; **(Suppl 5)**: 83–91.
24 Ogris M, Steinlein P, Kursa M, Mechtler K, Kircheis R, Wagner E. The size of DNA/transferrin-PEI complexes is an important factor for gene expression in cultured cells. *Gene Therapy* 1998; **5**: 1425–1433.
25 Mori Y, Nagaoka S, Takiuchi H, Kikuchi T, Noguchi N, Tanzawa H *et al*. A new antithrombogenic material with long polyethylene oxide chains. *Trans Am Soc Artif Intern Organs* 1982; **28**: 459–463.
26 Merrill EW, Salzman EW. Polyethylene oxide as a biomaterial. *ASAIO J* 1983; **6**: 60–64.
27 Llanos GR, Sefton MV. Does polyethylene oxide possess a low thrombogenicity? *J Biomater Sci Polym Ed* 1993; **4**: 381–400.
28 Amiji M, Park K. Prevention of protein adsorption and platelet adhesion on surfaces by PEO/PPO/PEO triblock copolymers. *Biomaterials* 1992; **13**: 682–692.
29 Llanos GR, Sefton MV. Immobilization of poly(ethylene glycol) onto a poly(vinyl alcohol) hydrogel: 2. Evaluation of thrombogenicity. *J Biomed Mater Res* 1993; **27**: 1383–1391.
30 Espadas-Torre C, Meyerhoff ME. Thrombogenic properties of untreated and poly(ethylene oxide)-modified polymeric matrices useful for preparing intraarterial ion-selective electrodes. *Anal Chem* 1995; **67**: 3108–3114.
31 Du H, Chandaroy P, Hui SW. Grafted poly(ethylene glycol) on lipid surfaces inhibits protein adsorption and cell adhesion. *Biochim Biophys Acta* 1997; **1326**: 236–248.
32 Pasche S, Voros J, Griesser HJ, Spencer ND, Textor M. Effects of ionic strength and surface charge on protein adsorption at PEGylated surfaces. *J Phys Chem B* 2005; **109**: 17545–17552.
33 Stary HC, Blankenhorn DH, Chandler AB, Glagov S, Insull Jr W, Richardson M *et al*. A definition of the intima of human arteries and of its atherosclerosis-prone regions. A report from the Committee on Vascular Lesions of the Council on Arteriosclerosis, American Heart Association. *Circulation* 1992; **85**: 391–405.
34 Guzman RJ, Lemarchand P, Crystal RG, Epstein SE, Finkel T. Efficient and selective adenovirus-mediated gene transfer into vascular neointima. *Circulation* 1993; **88**: 2838–2848.
35 Itaka K, Yamauchi K, Harada A, Nakamura K, Kawaguchi H, Kataoka K. Polyion complex micelles from plasmid DNA and poly(ethylene glycol)-poly(L-lysine) block copolymer as serum-tolerable polyplex system: physicochemical properties of micelles relevant to gene transfection efficiency. *Biomaterials* 2003; **24**: 4495–4506.
36 Ozaki Y, Satoh K, Yatomi Y, Yamamoto T, Shirasawa Y, Kume S. Detection of platelet aggregates with a particle counting method using light scattering. *Anal Biochem* 1994; **218**: 284–294.
37 Yamamoto T, Egawa Y, Shirasawa Y, Ozaki Y, Sato K, Yatomi Y *et al*. A laser light scattering *in situ* system for counting aggregates in blood platelet aggregation. *Meas Sci Technol* 1995; **6**: 174–180.
38 Tomida Y, Iino S, Nishikawa M, Hidaka H. A new system to detect native microaggregates of platelets *in vivo*, with a novel platelet aggregometer employing laser light scattering. *Thromb Res* 1998; **92**: 221–228.
39 Misawa Y, Konishi H, Fuse K. Platelet aggregates and cardiopulmonary bypass. *Ann Thorac Surg* 2001; **72**: 981–982.

Lipids (2007) 42:893–900
DOI 10.1007/s11745-007-3067-z

ORIGINAL ARTICLE

# Effects of Dietary Cholesterol on Tissue Ceramides and Oxidation Products of Apolipoprotein B-100 in ApoE-Deficient Mice

**Ikuyo Ichi · Yuka Takashima · Noriko Adachi · Kayoko Nakahara · Chiaki Kamikawa · Mariko Harada-Shiba · Shosuke Kojo**

Received: 1 March 2007 / Accepted: 20 April 2007 / Published online: 24 July 2007


**Abstract** Oxidized LDL (oxLDL) has been shown to activate the sphingomyelinase pathway producing ceramide in vascular smooth muscle cells. Therefore ceramide, which is a biologically active lipid causing apoptosis in a variety of cells, may be involved in the apoptotic action of oxLDL. In this study, we examined whether cholesterol enriched diets affected ceramide metabolism and oxidation product of LDL, represented by degradation of apolipoprotein B-100 (apoB) in apoE-deficient ($apoE^{-/-}$) mice. $ApoE^{-/-}$ and wild type mice were fed a standard (AIN-76) diet or 1% cholesterol-enriched diet for 8 weeks. Tissue ceramide levels were analyzed using electrospray tandem mass spectrometry (LC-MS/MS). Ceramide levels in the plasma and the liver of $apoE^{-/-}$ mice were intrinsically higher than those of the wild type. In $apoE^{-/-}$ mice, dietary cholesterol significantly increased several ceramides and degradation products of apoB in plasma compared to those fed the control diet. Dietary cholesterol did not affect tissue ceramide levels in the wild type mice. Based on these results, plasma ceramides possibly correlate with the increase in LDL oxidation and are a risk factor for atherosclerosis.

**Keywords** Ceramide · Cholesterol · Apolipoprotein B-100 · Oxidation · LC-MS/MS

I. Ichi · Y. Takashima · N. Adachi · K. Nakahara · C. Kamikawa · S. Kojo (✉)
Department of Food Science and Nutrition,
Nara Women's University, Nara 630-8506, Japan
e-mail: kojo@cc.nara-wu.ac.jp

M. Harada-Shiba
Department of Bioscience,
National Cardiovascular Center Research Institute,
Osaka 565-8565, Japan

**Abbreviations**

| | |
|---|---|
| ApoB | apolipoprotein B-100 |
| $ApoE^{-/-}$ | apoE deficient |
| IMT | Intima-media thickness of the carotid artery |
| LDL | Low-density lipoprotein |
| oxLDL | oxidized LDL |
| SDS-PAGE | Sodium dodecyl sulfate polyacrylamide gel electrophoresis |
| SM | Sphingomyelin |
| SMase | Sphingomyelinase |
| SPT | Serine palmitoyl-CoA transferase |
| TG | Triglyceride |

## Introduction

Ceramide has been implicated in regulating cell-cycle arrest, apoptosis, and cell senescence [1–3] and is reported to serve as an intracellular second messenger [4]. Therefore, ceramide has attracted much attention as a new lipid mediator. Ceramide consists of a fatty acid of C16–C26 chain length bound to the amino group of sphingosine. Ceramide is generated by sphingomyelin (SM) hydrolysis by sphingomyelinase (SMase) or by de novo synthesis starting from serine-palmitoyl transferase (SPT) [5]. A significant positive correlation was observed between plasma levels of SM and the severity of coronary heart disease [6], and plasma SM levels increased in human familial hyperlipidemias [7]. Recent studies have demonstrated correlations between sphingomyelin and atherogenic risk factors of plasma in humans [8] and inhibitions of de novo SM and ceramide biosynthesis reduced atherosclerotic lesion in $apoE^{-/-}$ mice [9, 10].

We recently showed that ceramide concentrations in human plasma had a significantly positive correlation with lipid markers that associated with atherosclerosis [11]. Plasma ceramide concentration increased drastically at a high level of LDL cholesterol (more than 170 mg/dL). Therefore, an increase in ceramide may be a risk factor for atherosclerosis, like LDL cholesterol.

Oxidative modification of LDL is an important factor in the development of atherosclerosis [12]. Although LDL is composed of lipids, protein, and sugar chains, studies on the oxidation of LDL have mainly focused on lipid peroxidation [13]. The protein part of LDL, apolipoprotein B-100 (apoB), is also reactive to radical oxidation and it undergoes fragmentation and conjugation [14, 15]. Among the plasma proteins, apoB is unusually reactive to radical reactions compared to albumin and transferrin and even comparable to vitamin E, a typical radical scavenger [14]. Thus, both fragmented and conjugated apoB proteins are present in normal human serum and these oxidation reaction products of LDL tend to increase with age [15]. In addition, we reported that B-ox, namely the sum of fragmented and conjugated apoB proteins determined by an immunoblot assay, showed a significant positive correlation with IMT (intima-media thickness of the carotid artery) and LDL cholesterol, and a negative correlation with HDL cholesterol, and vitamin C [15]. These reports suggest that B-ox is a reliable mechanism-based indicator of atherosclerosis.

Proteolytic degradation of apoB has been shown to cause aggregation and fusion of LDL [16]. Aggregated LDL in atherosclerotic lesions is proposed as representing a central process in atherosclerosis [17] and is enriched with ceramide [18]. Furthermore, LDL treated with SMase induces foam cell formation in vitro [18, 19]. Based on these reports, a correlation between ceramide and oxLDL is suggested.

Dietary cholesterol raises LDL cholesterol levels and a very high intake of cholesterol causes atherosclerosis. The activity of SPT, which catalyzes the first step in ceramide synthesis, is augmented in the aorta of rabbits fed high cholesterol diets [20]. Treatment of mice with myriocin, a specific inhibitor of SPT, lowered plasma cholesterol levels of ceramide in a dose-dependent manner. Therefore, high cholesterol diets may affect ceramide synthesis. The apoE$^{-/-}$ mice exhibit high levels of plasma cholesterol as a result of impaired clearance of cholesterol-enriched lipoproteins [21]. Therefore, apoE$^{-/-}$ mice are more sensitive to dietary cholesterol. In the present study, we examine the effect of high cholesterol diets on the ceramide levels in plasma, liver, and adipose tissues of apoE$^{-/-}$ mice in comparison with wild-type mice. We also demonstrate that dietary cholesterol results in enhancement of oxidation of apoB, namely degradation of apoB, in apoE$^{-/-}$ mice.

## Experimental Procedures

### Materials

All solvents were purchased from Wako Pure Chemicals Co. (Osaka, Japan). All other reagents were obtained from Funakoshi Co. (Tokyo, Japan). A commercially available diagnostic kit for cholesterol and triglyceride (TG) were purchased from Wako Pure Chem. Co. (Osaka, Japan). Silica gel 60 TLC plates were purchased from Merck (Darmstadt, Germany). A Vectastain ABC-PO (goat IgG) kit was purchased from Vector Lab. Inc. (Burlingame, CA, USA). Anti-human lipoprotein B goat IgG was purchased from Sigma Chem. Co. (St. Louis, MO, USA). Polyvinylidene difluoride (PVDF) membrane filters were purchased from Millipore (Tokyo, Japan). Electrophoresis reagents were purchased from Nacalai Tesque Inc. (Kyoto, Japan).

### Animals and Diets

This study was approved by the Animal Care Committee of Nara Women's University. Eight-week-old male apoE$^{-/-}$ mice on C57BL/6J background mice were purchased from Jackson Laboratories (Bar Harbor, Me., USA). Eight-week-old male C57BL/6J mice were also obtained from Japan SLC Co. (Hamamatsu, Shizuoka, Japan). The animals were housed in a room at 24 ± 2 °C, with a 12/12 h light–dark cycle. A standard diet was formulated according to the AIN-76 formula. The control group was fed a standard diet, and the cholesterol group was fed a standard diet supplemented with 1% cholesterol. Mice were randomized into the two groups. Mice were fed these experimental diets ad libitum for 8 weeks. All mice were starved for 6 h before killing.

### Analytical Method

Mice were anesthetized with Nembutal, and blood samples were collected by right-ventricle puncture using a syringe containing sodium heparin as an anticoagulant. After perfusion, the liver and adipose tissues were dissected out. Blood was centrifuged to separate the plasma.

Plasma cholesterol and TG were measured using a commercially available diagnostic kit. Liver cholesterol concentration was analyzed by gas–liquid chromatography (GC-2014, Shimadzu, Kyoto, Japan) using 5α-cholestane as an internal standard [22]. Liver TG was analyzed as described by Fletcher et al. [23]. Vitamin C was measured according to a specific and sensitive method involving chemical derivatization and HPLC [24].